EPJ manuscript No.
(will be inserted by the editor)

Study of medium-spin states of neutron-rich ^{87,89,91}Rb isotopes

D.A. Torres[1,2,a], R. Chapman[2], V. Kumar[2,b], B. Hadinia[2], A. Hodsdon[2], M. Labiche[2,c], X. Liang[2], D. O'Donnell[2], J. Ollier[2], R. Orlandi[2,d], J.F. Smith[2], K.-M. Spohr[2,e], P. Wady[2], Z.M. Wang[2], L. Corradi[3], E. Fioretto[3], A. Gadea[3], G. de Angelis[3], N. Mărginean[3,e], D.R. Napoli[3], E. Sahin[3,f], A.M. Stefanini[3], J.J. Valiente-Dobón[3], F.D. Vedova[3], M. Axiotis[3], T. Martinez[3], S. Szilner[4], D. Bazzacco[5], S. Beghini[5], E. Farnea[5], R. Mărginean[5,e], D. Mengoni[5], G. Montagnoli[5], F. Recchia[5], F. Scarlassara[5], C.A. Ur[5,e], S.M. Lenzi[5], S. Lunardi[5], T. Kröll[5,g], F. Haas[6], T. Faul[6], M. Hjorth-Jensen[7,8], B.G. Carlsson[9,h], S.J. Freeman[10], A.G. Smith[10], G. Jones[11], N. Thompson[11], G. Pollarolo[12], and G.S. Simpson[13]

[1] Departamento de Física, Universidad Nacional de Colombia, Bogotá, Colombia
[2] SUPA, School of Computing, Engineering, and Physical Sciences, University of the West of Scotland, Paisley, PA1 2BE, UK
[3] INFN-Laboratori Nazionali di Legnaro, Viale dell'Università 2, I-35020 Legnaro (Padova), Italy
[4] Ruđer Bošković Institute, Zagreb, Croatia
[5] INFN Sezione di Padova and Dipartimento di Fisica dell'Università, via F. Marzolo 8, I-35131 Padova, Italy
[6] Institut Pluridisciplinaire Hubert Curien, CNRS-IN2P3, Strasbourg, France
[7] National Superconducting Cyclotron Laboratory and Department of Physics and Astronomy, Michigan State University, East Lansing 48824 MI, USA
[8] Department of Physics and Center for Computing in Science Education, University of Oslo, N-0316 Oslo, Norway
[9] Department of Physics, University of Jyväskylä, P.O. Box 35 (YFL) FI-40014, Jyväskylä, Finland
[10] School of Physics and Astronomy, University of Manchester, Manchester, M13 9PL, UK
[11] Department of Physics, University of Surrey, Guildford, GU2 7XH, UK
[12] Dipartimento di Fisica Teorica, Università di Torino, and Istituto Nazionale di Fisica Nucleare, 10125 Torino, Italy
[13] Université Grenoble Alpes, CNRS, LPSC, Institut Polytechnique de Grenoble, IN2P3, F-38026 Grenoble, France

Received: date / Revised: date

Abstract. Excited states of the rubidium isotopes $^{87,89,91}_{37}$Rb have been studied at the INFN Legnaro National Laboratory. Measurements of the γ-ray decay of fragments produced in binary grazing reactions resulting from the interaction of a beam of 530 MeV ^{96}Zr ions with a ^{124}Sn target have been complemented by studies of the γ-ray decay of fission fragments produced in the interaction of a beam of 230 MeV ^{36}S ions with a thick ^{176}Yb target. The structure of the yrast states of $^{87,89,91}_{37}$Rb has been discussed within the context of spherical shell-model and cranked Nilsson-Strutinsky calculations.

[a] e-mail: datorresg@unal.edu.co
[b] *Present address:* Department of Physics and Astrophysics, University of Delhi, 110007, India.
[c] *Present address:* STFC Daresbury Laboratory, Warrington, WA4 4AD, UK.
[d] *Present address:* Advanced Science Research Center, Japan Atomic Energy Agency, Tokai, Ibaraki, 319-1195, Japan.
[e] *Present address:* Extreme Light Infrastructure (ELI-NP) & IFIN-HH, Horia Hulubei National Institute of Physics and Nuclear Engineering, Bucharest-Măgurele, RO-077125, Romania.
[f] *Present address:* Department of Physics, University of Oslo, P.O. Box 1048, Blindern, N-0316, Oslo, Norway.
[g] *Present address:* Institut für Kernphysik, Technische Universität Darmstadt, D-64289 Darmstadt, Germany.
[h] *Present address:* Department of Mathematical Physics, Lund Institute of Technology, S-22100 Lund, Sweden.

1 Introduction

The study of neutron-rich nuclei in the neighbourhood of mass number $A \sim 100$ has been the subject of growing interest in recent years, motivated by the onset of collectivity in the region and the goal of understanding the underlying microscopic structure. Since these nuclei lie on the pathway of the rapid neutron capture process (r-process) [1], there is also a nuclear astrophysical interest in the structure of such nuclei. The experimental study of medium to high-spin states in this region of the chart of nuclides has been advanced through γ-ray spectroscopy studies associated with the population of the nuclei of interest using binary grazing reactions [2–4], fusion-fission, and spontaneous fission reactions [5,6]. Recent studies of

even-even nuclei with $A \sim 100$ have explored the influence of the neutron ($h_{11/2}, g_{7/2}$) and proton ($g_{9/2}$) orbitals on the evolution of deformation [7,6]; however there is currently a lack of experimental information for odd-even nuclei with $N \geq 50$.

The region of the nuclear chart centred around mass number $A = 100$, between the $28 < Z < 50$ and $50 < N < 82$ major shell closures, is predicted to have large quadrupole deformation [8,9]. Within this area of the nuclear landscape, there is a well established region of large prolate deformation in the Sr and Zr isotopes, first observed experimentally in 1970 [10]. There is a sudden onset of quadrupole deformation at $N = 60$ in strontium ($Z = 38$) and zirconium ($Z = 40$); the energy of the first 2^+ state drops from 815 keV in $^{96}Sr_{58}$ to 144 keV in $^{98}Sr_{60}$ and from 1233 keV in $^{98}Zr_{58}$ to 212 keV in $^{100}Zr_{60}$ [11]. The sudden onset of deformation between $N = 58$ and $N = 60$ is quenched with increasing Z and this can be seen in the behaviour of the measured two-neutron separation energies as a function of neutron number for Z in the range from 36 to 45 [12]. For the odd-A isotopes of Rb, the calculations of Möller and Nix [8] predict a gradual increase in ground-state deformation from $^{92}Rb_{55}$ to $^{96}Rb_{59}$, with the deformation remaining essentially constant and large (ground-state electric quadrupole moment $\approx$ 2–3 b) from $^{97}Rb_{60}$ to $^{102}Rb_{65}$. Mean-square charge radii [13–15] and two-neutron separation energies [12,16] confirm a sudden structural change at $N = 60$. A recent Coulomb-excitation measurement [17] on neutron-rich $^{97}Rb_{60}$ and $^{99}Rb_{62}$ has provided the first strong experimental evidence for enhanced quadrupole collectivity through the observation of rotational sequences. In addition, an excited rotational band was observed in $^{96}Rb_{59}$ [18], providing evidence for shape coexistence. As will be seen later, theoretical calculations performed as part of the present work suggest the existence of shape coexistence in the lighter Rb isotopes. In contrast to the sudden onset of deformation at $N = 60$, for the lighter isotopes of Rb it is expected that, as neutrons are added to the $2d_{5/2}$ shell, there will be a tendency for the nucleus in its ground state to acquire a quadrupole deformation in order to remove the degeneracy associated with the occupancy of the $2d_{5/2}$ orbit; this is the nuclear analog of the Jahn-Teller effect [19,20]. There is indeed evidence from the systematic behaviour of the mean square charge radii of the ground states of the isotopes of $_{38}$Sr, $_{37}$Rb, and $_{36}$Kr that there are small departures from a spherical shape as the neutron number increases from $N = 50$ to $N = 58$. This is manifest in the slow increase of mean-square charge radii with increasing neutron number, measured in laser-spectroscopy experiments [13–15]. In the neighbouring isotones of $^{87}Rb_{50}$ with $Z = 36$ and 38, namely ^{86}Kr and ^{88}Sr, the energies of the first 2^+ excited states are large, 1564.6 keV and 1836.1 keV, respectively, as is expected for a spherical shell closure. For the neighbouring isotones of $^{89,91,93}Rb_{52,54,56}$ with $Z = 36$ and $Z = 38$, the first 2^+ energies are reasonably constant, about 1700 keV for the Kr isotopes and about 830 keV for the isotopes of Sr. For these isotopes of Kr and Sr, the ratio of the excitation energy of the first 4^+ state to that of the first 2^+ state lies in the range from 1.99 to 2.56. The increasing ratio with increasing neutron number may indicate a tendency towards a deformed shape as the $1d_{5/2}$ neutron shell is being filled. Indeed, in the isotopes of Kr, the $B(E2; 0^+ \rightarrow 2^+)$ values [21] increase from 7.7(8) W.u. for $^{88}Kr_{52}$ to 16.8(6) W.u. for $^{92}Kr_{56}$, indicating an increasing quadrupole collectivity with increasing neutron number. On the other hand, for the isotopes of Sr with $N = 52$, 54, and 56, the $B(E2; 0^+ \rightarrow 2^+)$ values [21] are subject to large experimental errors, namely $8.5^{+3.7}_{-2.0}$ W.u., $7.7^{+5.5}_{-2.3}$ W.u., and $7.8^{+5.2}_{-2.2}$ W.u., respectively, which makes it difficult to draw definitive conclusions about how collectivity changes with increasing occupancy of the $2d_{5/2}$ neutron orbit in this case.

To date, within the context of shell-model calculations, an effective two-body interaction, determined by fitting experimental data in the neutron-rich $A \sim 100$ region, has yet to be developed. Shell-model studies performed for nuclei in the region have involved restricted-basis shell-model calculations within a very large model space [22, 7,6,3,2], comprising the $\pi[1f_{5/2}, 2p_{3/2}, 2p_{1/2}, 1g_{9/2}]$ and $\nu[1g_{9/2}, 2d_{5/2}, 3s_{1/2}, 2d_{3/2}, 1g_{7/2}, 1h_{11/2}]$ orbitals.

Here, we present the results of experimental and theoretical studies of the medium-spin structure of the ^{87,89,91}Rb isotopes. The main aim of this work is the study of the evolution of the level structure with increasing neutron number and a comparison with shell-model (SM) calculations. In sect. 2, a description of the experiments is given. Experimental results are presented in sect. 3 and discussed within the context of the results of shell-model and Cranked Nilsson-Strutinsky (CNS) calculations in sects. 4 and 5, respectively. Finally, a summary appears in sect. 6.

2 Experimental procedure

Two experimental setups using beams delivered by the combination of the XTU-Tandem and ALPI accelerators at the INFN Legnaro National Laboratory have been used here for the study of neutron-rich nuclei in the $A \sim 100$ region. In the first experiment, a beam of ^{96}Zr ions at 530 MeV (5.52 MeV/nucleon) incident on a thin ^{124}Sn target was utilized to initiate binary grazing reactions. The target, which had a thickness of 300 μg cm^{-2}, was isotopically enriched to 94.6% and had a carbon backing of thickness 40 μg cm^{-2}. Projectile-like binary reaction fragments were detected by the PRISMA magnetic spectrometer [23, 24], at a laboratory grazing angle of 38° with respect to the beam direction, covering a solid angle of $\sim$ 80 msr (with angular acceptances of $\Delta\theta \sim 12°$ and $\Delta\phi \sim 22°$) and with a momentum acceptance of $\Delta p/p = \pm 10\%$. At the entrance to PRISMA, projectile-like ions are registered by a two-dimensional position-sensitive micro-channel plate (MCP) detector [25] providing a fast time signal for time-of-flight (ToF) and (x_i, y_i) initial position measurements. The ions then pass through quadrupole singlet and magnetic dipole elements, and are finally detected and identified at the focal plane detector system. This consists of a ten-section multiwire parallel-plate avalanche counter

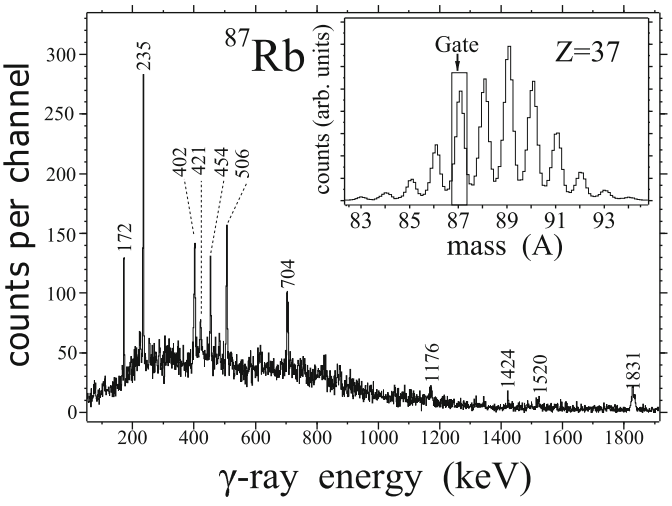

Fig. 1. Energy spectrum of γ rays detected in coincidence with the $A = 87$ mass for $Z = 37$ (^{87}Rb) identified at the focal plane of the PRISMA spectrometer. The inner panel shows the $Z = 37$ mass spectrum, and the gate at $A = 87$.

(MWPPAC) [26] providing a timing signal, in order to perform time-of-flight measurements in coincidence with the MCP, and (x_f, y_f) signals, followed by a 10×4 array of transverse-field multi-parametric Ionization Chambers (IC), which give the energy loss (ΔE) and the total energy (E) of the ions [25,26]. The mass resolution of PRISMA was $\Delta A/A = 1/190$, allowing a clean identification of the detected reaction products from $Z = 24$ (Cr) to $Z = 42$ (Mo). The associated γ rays from target- and projectile-like products were detected in coincidence using the CLARA [27] array of 25 escape-suppressed Ge Clover (EUROBALL-type) detectors. The detectors of the CLARA array form a hemisphere covering a large azimuthal angle range, between $\theta_{\rm CLARA} = 98.8°$ and $174.1°$, with respect to the entrance aperture of the PRISMA magnetic spectrometer. The CLARA array has a photopeak efficiency of about 3% and a peak-to-total ratio of 0.45 for ^{60}Co 1332 keV γ rays. Ion tracking through the PRISMA spectrometer together with time-of-flight measurements were used to determine the velocity vector of the projectile-like fragments and this allows the Doppler correction of γ-ray energies to be performed on an event-by-event basis [28]. The statistics in the experiment were not adequate to perform a γ-γ coincidence analysis. In the discussion below, we will refer to this setup as the PRISMA/CLARA experiment. Figure 1 shows an example of the quality of the data from the experiment; the mass spectrum of rubidium isotopes ($Z = 37$) is shown in the inner figure. It is possible to identify masses from $A = 83$ to $A = 94$. The main figure shows the associated γ-ray spectrum obtained by gating on mass $A = 87$ (^{87}Rb).

Data from the PRISMA/CLARA experiment permit the unambiguous identification of γ rays associated with the decay of excited states of rubidium isotopes of a specific mass number. In addition, measurements of γ-ray multipolarity are possible based on γ-ray asymmetry ratios, defined as $R_{\rm asym} = I_\gamma(\theta_1)/I_\gamma(\theta_2)$. Here $I_\gamma(\theta_1)$ and $I_\gamma(\theta_2)$ are the intensities of the same γ-ray transition measured in any of the detectors at $\theta_1 = 98.8°$, while $98.8° \leq \theta_2 \leq 174.1°$; θ_i corresponds to the angle between the Clover detector and the centre of the entrance aperture of the PRISMA spectrometer. Typical $R_{\rm asym}$ values of 1.3 and 0.7 are expected for stretched quadrupole and dipole transitions, respectively [30].

While the PRISMA/CLARA experiment enables the unambiguous assignment of γ-ray transitions to each rubidium isotope studied here, the reaction yield was insufficient to allow the production of γ-ray coincidence matrices from which reliable level schemes can be constructed. However, γ-γ and γ-γ-γ coincidence data were available from a thick target experiment carried out using the Ge multi-detector array GASP in configuration I. The array consists of 40 escape-suppressed coaxial hyperpure germanium detectors and an 80 element inner BGO ball for γ-ray multiplicity and total-energy measurements. The total photopeak efficiency of the Ge array is about 3% at a γ-ray energy of 1332 keV (^{60}Co), and the mean peak-to-total ratio is about 60–65% at 1332 keV for the Compton-suppressed γ-ray spectra [31]. In the second experiment, a beam of ^{36}S ions at an energy of 230 MeV (6.39 MeV/u) was delivered onto a thick target of ^{176}Yb. The target was isotopically enriched to 97.8% and was of thickness 14 mg cm^{-2} with an isotopically enriched ^{208}Pb (98.7%) backing of thickness 35 mg cm^{-2}; the backing was sufficiently thick to stop all forward-moving reaction products. The fusion-fission reaction with the beam and target combination populates nuclei in the region of interest [32]. Data from the GASP experiment were used to establish coincidence relationships between γ rays through the analysis of γ-γ and γ-γ-γ coincidence matrices and cubes. In the discussion below, we will refer to this setup as the GASP experiment.

The GASP data were also used in the measurement of γ-ray angular correlations for ^{87}Rb and ^{89}Rb; however, the statistics were not sufficiently good to measure angular correlations for ^{91}Rb. When two consecutive γ rays, namely γ_0 and γ_1, are detected by any pair of GASP detectors separated by an angle θ, the angular distribution of the radiation is described by the function $\mathrm{W}(t_0, t_1, \theta) = \sum_\lambda^{\lambda_{\rm max}} q_\lambda A_{\lambda\lambda}(t_0, t_1) P_\lambda(\cos\theta)$ [33], where t_0 (t_1) denotes the properties of the γ-ray transition γ_0 (γ_1). The coefficients $A_{\lambda\lambda}$ are tabulated in ref. [34], and the attenuation coefficients q_λ were calculated following the procedure of ref. [33]. For the GASP array in configuration I, these values are $q_0 = 1.0$, $q_2 = 0.909$ and $q_4 = 0.602$. The coefficients take into account the effect of the finite size of the Ge detectors, and the effects of choosing $\pm 10°$ as the allowed range for the separation angle between pairs of detectors. Two-fold γ-ray coincidences were sorted into three two-dimensional matrices. For the first matrix, the first and second γ rays correspond to their detection in two Ge detectors with a separation angle of $\theta_s = 90° \pm 10°$. The second matrix corresponds to γ rays observed in a pair of detectors with $\theta_s = 120° \pm 10°$ and $60° \pm 10°$, while, for the third matrix, $\theta_s = 150° \pm 10°$ and $30° \pm 10°$. The matrices contained approximately 4×10^9, 9×10^9, and 5×10^9

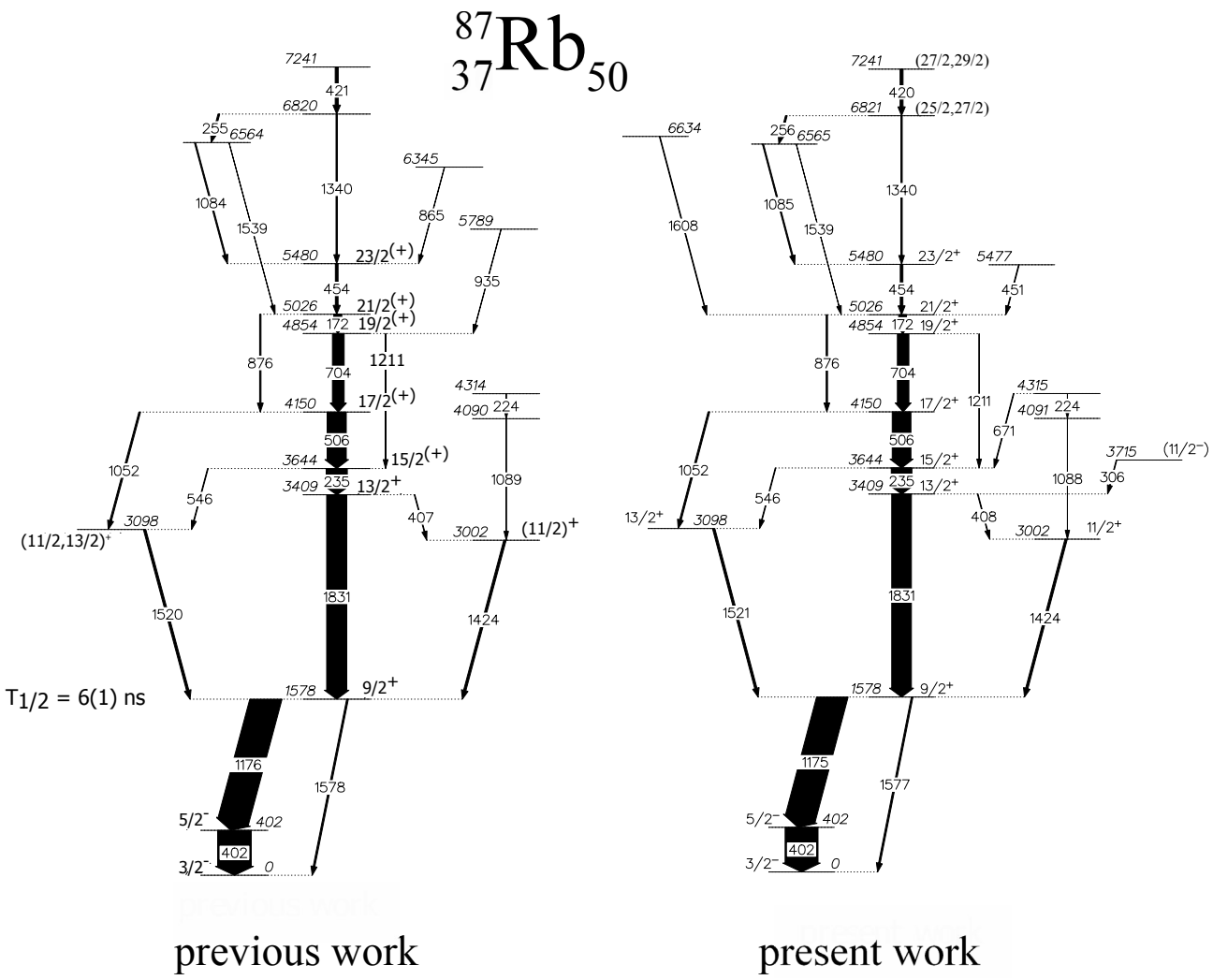

Fig. 2. Partial level schemes of ^{87}Rb. The level scheme corresponding to previous work is based on refs. [22,29]. Energies are in units of keV, given to the nearest integer value, and the widths of the arrows are proportional to the relative intensities of the γ-ray transitions. Measured γ-ray energies are presented in table 1. See text for details.

events, respectively. For a specific cascade $I_0 \xrightarrow{\gamma_0} I_1 \xrightarrow{\gamma_1} I_2$, where I_0, I_1, and I_2 are the spins of the initial, intermediate, and final states, a gate on γ_1 was made on the first axis of the three matrices and, for each projected one-dimensional γ-ray spectrum, the number of γ_0 counts was obtained. This gives the quantities $N(90°)$, $N(120°)$, and $N(150°)$, which were then normalized. The normalization factors were obtained through an angular correlation analysis of known stretched $E2$-$E2$ and $E1$-$E2$ cascades in adjacent even-even nuclei (^{88}Sr, ^{104}Ru, and ^{100}Mo); the results of ref. [34] were used in the normalization procedure. The normalized yields, $N(\theta)$ (normalized to unity at 90°), were fitted to $W(t_0, t_1, \theta)$ to obtain the coefficients $A_{\lambda\lambda}/A_{00}$, which can be compared to the predicted values given in ref. [34]. Where possible, the assigned γ-ray multipolarities were determined by combining the results of the angular correlation measurements from the Gasp experiment with the asymmetry ratios from the Prisma/Clara experiment. Previously determined multipolarities, where available, are also presented.

3 Experimental results

The partial level schemes of ^{87,89,91}Rb nuclei from the present work, shown in figs. 2, 4, and 8, respectively, are informed by published work, and based on γ-ray coincidence relations, intensity balance considerations, transition energy relations, and by the observation that binary grazing reactions [35–38] and fusion-fission reactions [5] preferentially populate yrast and near-yrast states. The level energies, the corresponding depopulating γ-ray energies, relative γ-ray intensities, asymmetry ratios, proposed multipolarity, and spin and parity assignments are summarised in tables 1, 3, and 5 for ^{87}Rb, ^{89}Rb, and ^{91}Rb, respectively. Transition multipolarities from recent nuclear data evaluations and from other published works are presented in the final column of each table. The angular correlation coefficients for ^{87}Rb and ^{89}Rb are presented in tables 2 and 4, respectively. Not all known levels of ^{87,89,91}Rb are shown in figs. 2, 4, and 8. Low-spin non-yrast states are, in general, not populated in the present work and are not included in the level schemes presented here.

Table 1. The energies of excited states of ^{87}Rb (E_i) together with transition energies (E_γ) and relative intensities (I_γ) of γ rays placed in the level scheme, asymmetry ratios (R_{asym}), and the proposed multipolarities, spins and parities of the initial and final states. Multipolarities from the recent compilation by Johnson *et al.* [39] are given in the final column. See text for details. Relative intensities are based on the results of the GASP experiment. Quantities in italics correspond to new level energies or to hitherto unobserved γ-ray transitions.

E_i (keV)	E_γ (keV)	I_γ	R_{asym}	Proposed mult.	J_i^π	$\rightarrow$	J_f^π	Multipolarity [39]
402.5(2)	402.5(2)	100(4)	0.93(18)	$M1/E2$	$5/2^-$	$\rightarrow$	$3/2^-$	$M1/E2$
1577.7(4)	1175.4(4)	93(3)		$(M2)$	$9/2^+$	$\rightarrow$	$5/2^-$	$M2$
	1577.4(5)	5(2)		$(E3)$	$9/2^+$	$\rightarrow$	$3/2^-$	$(E3)$
3001.6(5)	1423.8(4)	7(2)	0.76(28)	$M1/E2$	$11/2^+$	$\rightarrow$	$9/2^+$	
3097.9(6)	1520.6(5)	7(2)	1.29(22)	$E2$	$(13/2^+)$	$\rightarrow$	$9/2^+$	
3409.1(5)	407.5(2)	2(1)			$13/2^+$	$\rightarrow$	$11/2^+$	
	1831.0(9)	86(4)	1.29(13)	$E2$	$13/2^+$	$\rightarrow$	$9/2^+$	
3643.9(5)	234.8(2)	62(2)	1.10(17)	$M1/E2$	$15/2^+$	$\rightarrow$	$13/2^+$	dipole + quadrupole
	546.5(3)	2(1)			$15/2^+$	$\rightarrow$	$13/2^+$	
3715.2(6)	*306.1(2)*	2(1)				$\rightarrow$	$13/2^+$	
4090.7(6)	1088.5(4)	< 1				$\rightarrow$	$11/2^+$	
4150.2(6)	506.4(3)	57(2)	0.96(16)	$M1/E2$	$17/2^+$	$\rightarrow$	$15/2^+$	dipole + quadrupole
	1051.7(4)	5(1)			$17/2^+$	$\rightarrow$	$13/2^+$	
4314.9(6)	224.1(2)	< 1				$\rightarrow$	$(15/2^+)$	
	671.4(3)	2(1)				$\rightarrow$	$15/2^+$	
4854.5(6)	704.1(3)	35(2)	0.91(19)	$M1/E2$	$19/2^+$	$\rightarrow$	$17/2^+$	dipole + quadrupole
	1211.0(4)	1(1)			$19/2^+$	$\rightarrow$	$15/2^+$	
5026.1(6)	171.6(2)	23(2)	0.95(19)	$M1/E2$	$21/2^+$	$\rightarrow$	$19/2^+$	dipole + quadrupole
	875.9(3)	4(2)			$21/2^+$	$\rightarrow$	$17/2^+$	
5476.8(7)	*450.8(2)*	2(1)			$(23/2^+)$	$\rightarrow$	$21/2^+$	
5480.5(6)	454.4(2)	8(1)	0.95(24)	$M1/E2$	$23/2^+$	$\rightarrow$	$21/2^+$	dipole + quadrupole
6565.5(7)	1085.3(4)	4(1)				$\rightarrow$	$23/2^+$	
	1539.3(5)	< 1				$\rightarrow$	$21/2^+$	
6634.2(8)	*1608.2(5)*	2(1)				$\rightarrow$	$21/2^+$	
6821.0(7)	255.6(2)	5(1)			$(25/2, 27/2)$			
	1340.1(4)	4(1)			$(25/2, 27/2)$	$\rightarrow$	$23/2^+$	
7241.4(7)	420.4(2)	9(1)	0.65(26)	$M1/E2$	$(27/2, 29/2)$	$\rightarrow$	$(25/2, 27/2)$	

Table 2. γ-ray angular correlations for two consecutive γ rays in a cascade in ^{87}Rb. See text for details.

E_0 (keV)	E_{γ_0} (keV)	$E_{\gamma_1}^a$ (keV)	A_{22}/A_{00}	A_{44}/A_{00}	Proposed multipolarity	
					γ_0	γ_1
4855	704	506	$-0.20(0.06)$	0.11(0.14)	$M1/E2$	$M1/E2$
5026	172	704	$-0.17(0.07)$	0.08(0.17)	$M1/E2$	$M1/E2$
5480	454	172	$-0.30(0.15)$	$-0.07(0.11)$	$M1/E2$	$M1/E2$

[a] The gates were performed in γ_1.

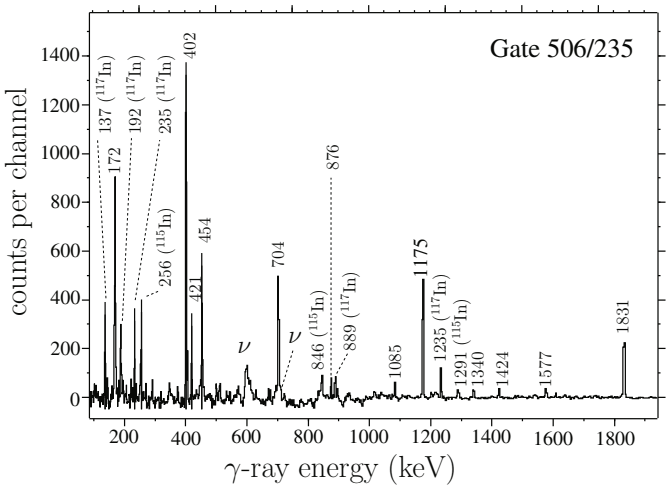

Fig. 3. Double-gated γ-ray spectrum for ^{87}Rb corresponding to gates set at 506 and 235 keV. Transitions corresponding to the partner fission fragments, ^{115}In and ^{117}In, are labelled. The data were taken with the GASP array. Neutron peaks are labelled with the symbol ν.

Thus, for example, the low lying excited states of ^{87}Rb at excitation energies of 845 keV ($J^\pi = 1/2^-$), 1349 keV (J^π unknown), 1389 keV ($J^\pi = 3/2^-$), and 1463 keV ($J^\pi = 1/2^-$) [39] are not included in the level scheme of fig. 2.

3.1 Levels and transitions in ^{87}Rb

The nucleus ^{87}Rb, with neutron number 50, is a semi-magic nucleus. The neutron shell gap here is of the order of 4.5 MeV [40] and, consequently, the low-energy region of the level scheme is expected to be described in terms of the occupation of the $1f_{5/2}$, $2p_{3/2}$, $2p_{1/2}$, and $1g_{9/2}$ proton shell-model orbits by the nine extra-core ($Z = 28$) protons and an inert neutron closed-shell core. The ground state, as expected from the shell-model orbits available above $Z = 28$, has a J^π value of $3/2^-$, corresponding to the occupation of the $2p_{3/2}$ orbital by three protons. On the same basis, we would expect the first excited $5/2^-$ state at an excitation energy of 402 keV to correspond to the four-particle one-hole configuration $\pi(1f_{5/2})^{-1}(2p_{3/2})^4$, the non-yrast $1/2^-$ state at $E_x = 845$ keV, unobserved in the present work, to correspond to the configuration $\pi(2p_{1/2})^1(2p_{3/2})^2$, and the first $9/2^+$ state at $E_x = 1134$ keV to correspond to the occupation of the $1g_{9/2}$ orbital by the odd proton. Proton pickup and stripping reactions [41–44] are consistent with the above description of the structure of the states. The spectroscopic factors, C^2S, for proton stripping to the $3/2^-$, $1/2^-$, and $9/2^+$ states are 0.34, 1.02, and 0.99, respectively. The $J^\pi = 5/2^-$ state at 402 keV is also populated in proton stripping, contrary to the simple shell-model description of the $^{86}_{36}$Kr ground state configuration. This indicates that $^{86}_{36}$Kr has, in its ground state, components of the form $\pi(2p_{3/2})^4\ (1f_{5/2})^{-2}$. Higher-lying excited states, and especially those of high spin, are expected to have components in their wave functions corresponding to promotion of one or more neutrons across the $N = 50$ shell gap.

The shell-model calculations which will be presented here, in sect. 4 of the paper, do not allow neutrons (protons) to cross the $N = 50$ ($Z = 50$) gap; consequently, one should expect to observe a significant disagreement between experiment and shell model with increasing excitation energy and increasing spin, which might reasonably be interpreted as corresponding to the onset of *np-nh* neutron correlations (where *np* stands for number of particles and *nh* the number of holes). Such correlations correspond to the breaking of the $N = 50$ neutron core.

The low-spin states of ^{87}Rb have been studied in β decay [45,46], in Coulomb excitation [47], in inelastic hadron scattering [48–50], in single-proton transfer reactions [41–44], and in a $(\gamma, \gamma\prime)$ experiment [51]. The experimental study of medium-high spin yrast and near-yrast states above the previously known $J^\pi = 9/2^+$ isomeric state at $E_x = 1578$ keV has, more recently, been carried out using fusion-fission and multinucleon transfer reactions. Three fusion-fission experiments involving the projectile-target combinations of ^{24}Mg + ^{176}Yb at 134.5 MeV, ^{23}Na + ^{176}Yb at 129 MeV, and ^{18}O + ^{208}Pb at 91 MeV [29] were used to populate a range of nuclei, including ^{87}Rb; the γ-ray decay of the final nuclei was studied using the GAMMASPHERE Ge multi-detector array of escape-suppressed Ge detectors. States of ^{87}Rb were populated up to an excitation energy of 7241 keV. Multinucleon transfer reactions initiated by the interaction of a beam of 460 MeV ^{82}Se ions with a thick target of ^{192}Os have also been used to populate states of ^{87}Rb up to an excitation energy of 6822 keV [22]; in this experiment, the γ-ray decay of the binary reaction fragments was measured using the GASP array. A recent evaluation of experimental data for the known nuclides of mass number 87 has also recently been published [39]. In relation to the structures above the isomeric state, the results from the present work agree, with few exceptions, with previous works, and a few new transitions have been added to the level scheme. As discussed earlier, fusion-fission and multinucleon transfer reactions selectively populate yrast and near-yrast states; consequently the states populated directly do not normally correspond to those populated in other processes, such as β decay and single nucleon transfer reactions.

The proposed level scheme based on the present work is presented in fig. 2, together with the level scheme based on refs. [22,29]. The energy levels in fig. 2, corresponding to previous published work, are those of Fotiades *et al.* [29]. The work of Zhang *et al.* [22] extended the previously known level scheme above the $9/2^+$ isomer to the 6822 keV level. The subsequent study by Fotiades *et al.* [29] added further to the level scheme. Multipolarity assignments made by Zhang *et al.* [22] were based on the measurement of angular distribution ratios from oriented states (ADO) and on the observed decay branches. On the other hand, Fotiades *et al.* [29] suggested spin and parity assignments for four levels above the isomer (at excita-

tion energies of 3002, 3098, 3409, and 3644 keV) which were based on a comparison with the excited states of ^{85}Kr and ^{89}Y above the $9/2^+$ isomer and on a comparison with shell-model calculations for ^{87}Rb. The assignments here agree with those of Zhang *et al.* In fig. 2, the spin and parity assignments above the $9/2^+$ isomer and corresponding to the previous work are those of Zhang *et al.*, where available; for the $E_x = 3098$ keV state the J^π value is that of Fotiades *et al.* [29]. In table 1, the measured γ-ray energies and relative intensities are based on the results of the GASP experiment. Here, the focus of discussion will be related mainly to the level structure above the isomeric state.

As mentioned above, fig. 1 shows a γ-ray spectrum from the PRISMA/CLARA experiment corresponding to the population of ^{87}Rb. An example of a double-gated γ-ray spectrum from the GASP experiment is presented in fig. 3; the gates in this case were set on the photopeaks at energies of 506 keV and 235 keV. The coincidence relationships between ^{87}Rb γ rays were established from such high-quality double-gated spectra.

As noted earlier, the state at $E_x = 1578$ keV with $J^\pi = 9/2^+$ is isomeric, with a half-life of 6(1) ns [50]. In the PRISMA/CLARA experiment, ^{87}Rb ions ($v/c \sim 9.7\%$) travel a distance of about 17 cm from the target position in 6 ns. Consequently, due to the isomerism of the decaying state, the measured intensity of the 1175 keV transition (and of the subsequent 402 keV transition) is considerably reduced in relation to the number of emitted γ rays. The spectroscopic factor for population of the state in the direct single-proton transfer reaction, ^{86}Kr(^{3}He, d)^{87}Rb, is 0.99 [43], as noted earlier, and this indicates that the state has a pure proton $1g_{9/2}$ configuration. The $\pi(1g_{9/2})$ state is also observed in the other $N = 50$ isotones, ^{89}Y [52] and ^{85}Br [53]. In ^{89}Y, the $9/2^+$ state appears at an excitation energy of 909 keV and the measured half life is 15.663(5) s [54]. The spectroscopic factor, measured in the ^{88}Sr(^{3}He, d)^{89}Y proton stripping reaction, is $C^2S = 0.74$, again indicating that the state is a fairly pure single proton $1g_{9/2}$ excitation. ^{84}Se is not a stable nucleus and the ^{84}Se(^{3}He, d)^{85}Br proton stripping reaction has not been reported in the literature to date. However, the ^{86}Kr(d,^{3}He)^{85}Br proton pickup reaction has been studied by May and Lewis [55] and by Pfeiffer *et al.* [56]. Within the context of the simple shell model, the $1g_{9/2}$ proton orbital is empty in the ^{86}Kr ground state and, consequently, no $\ell = 4$ proton pickup strength should be observed. Contrary to this expectation, $\ell = 4$ strength was observed by May and Lewis [55] for an excited state of ^{85}Br at $E_x = 2.310(31)$ MeV with a spectroscopic strength of $C^2S = 1.12$, corresponding to a proton $1g_{9/2}$ occupation probability of ${V_j}^2 = 0.11$ in the ground state of ^{86}Kr. However, a subsequent measurement by Pfeiffer *et al.* [56], which used a beam of vector-polarised deuterons, assigned a J^π of $3/2^-$ to a state at 2.3 MeV. In the 2014 evaluation of $A = 85$ nuclides by Singh and Chen [54], which post-dates the two above mentioned ^{86}Kr(d,^{3}He) studies, a J^π of $3/2^-$ has been assigned to a state at $E_x = 2.310(31)$ MeV on the basis of the work of Pfeiffer *et al.* [56]. An excited state at $E_x = 1859$ keV is a possible candidate for the $\pi(1g_{9/2})$ state of ^{85}Br [54] and the state has tentatively been included in a study of the systematics of the $\pi(1g_{9/2})$ orbital in the ^{78}Ni region by Bączyk *et al.* [57]. For the isotopes of Rb, Br, and As, the excitation energies of the lowest $9/2^+$ state relative to the first $5/2^-$ state show a minimum near neutron number 42. The isomeric state in ^{87}Rb is connected to the $5/2^-$ state by an $M2$ transition of energy 1175 keV, and to the ground state by a weak 1577 keV $E3$ transition. The branch to the ground state was first identified by Fotiades *et al.* [29]. The $B(M2; 9/2^+ \rightarrow 5/2^-)$ value of 0.12(2) W.u. is not particularly hindered, but nevertheless is in agreement with the range of hindrance factors for $M2$ transitions in this mass region [58,59]. The measured ratio $I_\gamma(1578\,\text{keV} \rightarrow 0\,\text{keV})/I_\gamma(1578\,\text{keV} \rightarrow 402\,\text{keV})$ of 0.12 ± 0.01 [39] has been combined with the known lifetime of the state at $E_x = 1578$ keV in a determination of $B(E3; 1578\,\text{keV} \rightarrow 0\,\text{keV})$. The resulting value, 0.89(0.16) $e^2\,fm^6$ (1.98(0.36) W.u.), falls within the distribution of $E3$ strength for nuclei in the mass region [58, 59]. There is a close-lying state at $E_x = 1578.0$ keV ($J^\pi = 1/2^-, 3/2^-$) [39], with energy separation from the $9/2^+$ state of only 0.1 keV, which has been populated in β decay from ^{87}Kr [45,46,39], in the ^{87}Rb(γ,γ') reaction [51], and in the ^{88}Sr(d,^{3}He) proton pickup reaction [41,42,44]; the state also decays both to the ground state and to the 402 keV first excited state. Since the state is non-yrast, its population in the present work is not expected.

We now comment on those transitions observed here for the first time and on transitions for which we are able to propose multipolarity assignments. No definitive parity assignments are possible from the present results; suggested electric or magnetic multipolarity assignments are therefore tentative. Multipolarity assignments have previously been proposed [39], see column 7 of table 1, for the transitions of energy 171.6, 234.8, 402.5, 454.4, 506.4, 704.1, 1175.4, and 1577.4 keV. Within the positive parity decay sequence based on the $J^\pi = 9/2^+$ isomeric state, the transitions for which assignments have previously been made (at energies of 234.8, 506.4, 704.1, 171.6, and 454.4 keV) are of mixed dipole/quadrupole multipolarity. The measured γ-ray asymmetry ratios from the present work (column 4 of table 1), although subject to large statistical uncertainty, are consistent with these earlier assignments. Based on these multipolarity assignments, the proposed J^π values of the states with excitation energies of 3409, 3644, 4150, 4854, 5026, and 5480 keV are $13/2^+$, $15/2^+$, $17/2^+$, $19/2^+$, $21/2^+$, and $23/2^+$ respectively, in agreement with the proposed assignments of Zhang *et al.* [22]. The multipolarity of the 1340.1 keV transition is unknown; consequently the J^π value of the 6821 keV level cannot be assigned. The most probable spin values, based on the population characteristics of the reactions used here, are (25/2) or (27/2). The 420.4 keV transition has a measured asymmetry consistent with a dipole multipolarity and it can therefore be speculated that the spin of the 7241 keV state is (27/2) or (29/2). It is noted again that the proposed assignments have been influenced

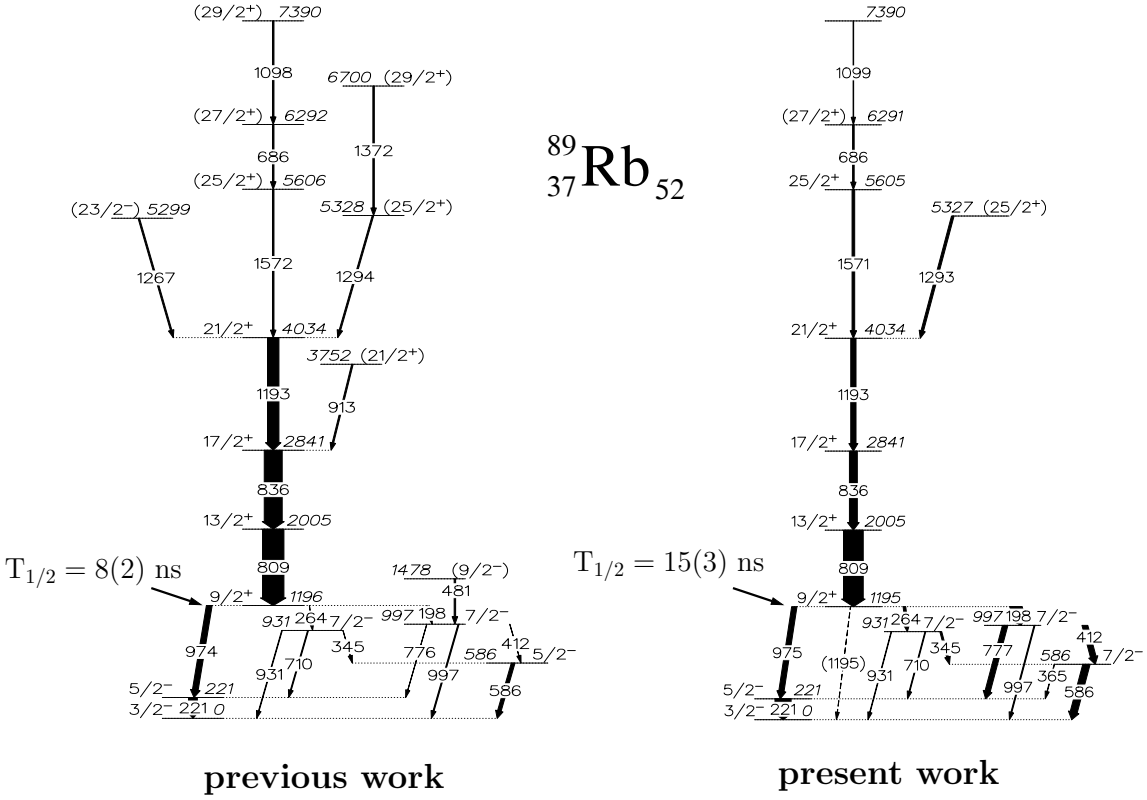

Fig. 4. Partial level scheme of ^{89}Rb. The level scheme corresponding to previous work is based on refs. [3,60,61]. Energies are in units of keV, given to the nearest integer value, and the widths of the arrows are proportional to the relative intensities of the γ-ray transitions. Measured γ-ray energies are presented in table 3. See text for details.

by the observation that fusion-fission reactions favour the population of yrast and near-yrast states. The 1831.0 keV transition which connects the $13/2^+$ state at 3409 keV to the $9/2^+$ isomeric state has a measured asymmetry which is consistent with a quadrupole transition, in agreement with the previously proposed spin values of the states. Finally, the transitions of energy 1423.8 keV and 1520.6 keV which feed the $9/2^+$ state have measured asymmetries consistent with mixed dipole/quadrupole and quadrupole, respectively, consistent with the J^π values of fig. 2. The angular correlation results presented in table 2 are consistent with these suggested multipolarities. The $M2$ multipolarity assignment of the 1175 keV transition is based on the lifetime of the $9/2^+$ isomeric state, discussed earlier. The proposed $E3$ multipolarity of the 1577 keV transition, also discussed above, is based on the J^π values of the two states connected by the transition.

The transition of energy 306 keV which populates the $13/2^+$ state at $E_x = 3409$ keV is reported here for the first time. The $E_x = 3707(8)$ keV state was populated in an $L = 4$ transition in a ^{87}Rb(p,p') experiment [48], suggesting a J^π value of $11/2^-$; we presume that this is the same state observed here at $E_x = 3715$ keV, which has tentatively, in fig. 2, been assigned a J^π value of $(11/2^-)$. The γ-ray transitions at 671 keV, 451 keV, and 1608 keV are reported here for the first time. It was not possible to identify transitions above the level at $E_x = 7241$ keV. In ref. [29] 865 keV and 935 keV transitions from the levels at $E_x = 6345$ keV and 5789 keV, respectively, were reported; these transitions are not observed in the present work.

3.2 ^{89}Rb experimental results

On the basis of the simple shell model, we expect the ground state of ^{89}Rb to be described in terms of the configuration

$$\pi[(1f_{5/2})^6(2p_{3/2})^3(2p_{1/2})^0(1g_{9/2})^0] \otimes \nu[(1g_{9/2})^{10}(2d_{5/2})^2(3s_{1/2})^0(2d_{3/2})^0(1g_{7/2})^0].$$

Low-lying excited states correspond to the occupation of the fpg-shell by the nine extra-core protons and rearrangement of the two extra-core neutrons within the sdg shell. Within the context of the shell-model calculations presented here, and based on these configurations, it is expected that high-spin states of ^{89}Rb will be described more accurately than was the case for ^{87}Rb, where promotion of neutrons across the $N = 50$ shell gap is not allowed. As we shall see later, this is indeed the case.

A study of the excited states of ^{89}Rb was recently carried out by Astier *et al.* [60], by Bucurescu *et al.* [3], and by Pawlat *et al.* [61]. An evaluation of $A = 89$ nuclides has also recently been undertaken by Singh and Chen [54]. The work of Astier *et al.* [60] post-dates the

Table 3. The energies of excited states of ^{89}Rb (E_i) together with transition energies (E_γ) and relative intensities of γ rays (I_γ) placed in the level scheme, based on the results of the GASP experiment, and asymmetry ratios (R_{asym}). Proposed multipolarities, based on the present work, appear in column five of the, followed by the proposed spins and parities of the initial and final states. The final column presents multipolarity assignments from the recent evaluation by Singh [54] and by Astier *et al.* [60] (in bold font).

E_i (keV)	E_γ (keV)	I_γ	R_{asym}	Proposed mult.	J_i^π	→	J_f^π	Multipolarity [54,60]
220.80(16)	220.90(20)	43(3)	1.06(17)	$M1/E2$	$5/2^-$	→	$3/2^-$	$M1$ **dipole**
585.85(18)	365.00(20)	2(1)			$5/2^-$	→	$5/2^-$	
	585.9(3)	30(3)	1.38(42)	$E2$	$5/2^-$	→	$3/2^-$	$E2$ **dipole**
931.32(24)	345.3(10)	17(3)	0.91(08)	$M1/E2$	$7/2^-$	→	$5/2^-$	
	710.4(3)	4(2)	1.01(28)	$M1/E2$	$7/2^-$	→	$5/2^-$	
	931.3(10)	3(1)			$7/2^-$	→	$3/2^-$	
997.47(18)	411.60(20)	16(3)	1.13(50)	$M1/E2$	$7/2^-$	→	$5/2^-$	$M1$ **dipole**
	777.2(3)	10(3)			$7/2^-$	→	$5/2^-$	
	997.2(3)	25(3)	1.14(47)	$E2$	$7/2^-$	→	$3/2^-$	
1195.48(21)	198.10(20)	60(3)			$9/2^+$	→	$7/2^-$	($E1$) **dipole**
	264.10(20)	13(3)			$9/2^+$	→	$7/2^-$	
	974.6(3)	27(3)		$M2$	$9/2^+$	→	$5/2^-$	($M2$) **quadrupole**
2004.6(4)	809.1(3)	100(7)	1.22(17)	$E2$	$13/2^+$	→	$9/2^+$	$E2$ **quadrupole**
2840.6(5)	836.0(3)	71(6)	1.16(22)	$E2$	$17/2^+$	→	$13/2^+$	$E2$ **quadrupole**
4033.5(6)	1192.9(4)	39(4)	1.37(27)	$E2$	$21/2^+$	→	$17/2^+$	$E2$ **quadrupole**
5326.6(7)	1293.1(4)	6(2)			$25/2^+$	→	$21/2^+$	
5605.0(7)	1571.5(5)	18(3)	1.15(25)	$E2$	$(25/2^+)$	→	$21/2^+$	
6291.0(7)	686.0(10)	17(3)	0.63(17)	$M1$	$(27/2^+)$	→	$(25/2^+)$	
7390.9(7)	1098.9(4)	8(2)				→	$(27/2^+)$	

Table 4. γ-ray angular correlations for two consecutive γ rays in a cascade in ^{89}Rb.

E_0 (keV)	γ_0 (keV)	γ_1^a (keV)	A_{22}/A_{00}	A_{44}/A_{00}	Proposed multipolarity	
					γ_0	γ_1
997.47(18)	411.60(20)	585.9(3)	0.00(0.02)	−0.014(0.06)	$M1/E2$	$E2$
931.32(24)	777.2(3)	220.90(20)	0.03(0.02)	0.00(0.09)	$M1/E2$	$M1/E2$
4033.5(6)	1192.9(4)	809.1(3)	0.11(0.02)	0.00(0.06)	$E2$	$E2$
5326.6(7)	1293.1(4)	1192.9(4)	0.11(0.02)	0.01(0.8)	$E2$	$E2$
5605.0(7)	1571.5(5)	1192.9(4)	0.08(0.05)	−0.05(0.08)	$E2$	$E2$

[a] The gates were set on γ_1.

evaluation. In the work of Bucurescu *et al.*, ^{90}Zr projectiles incident on a ^{208}Pb target and ^{82}Se projectiles incident on a target of ^{238}U were used to populate the final nuclei in binary grazing reactions; projectile-like species were detected and identified using the PRISMA magnetic spectrometer at the INFN Legnaro National Laboratory. The γ-ray decay of the binary reaction fragments was measured using the CLARA multi-detector Ge γ-ray array. Double and triple γ-ray coincidences were obtained using an additional thick target experiment which involved a beam of ^{82}Se ions incident on a target of ^{192}Os; the production of the ^{89}Rb isotope was again via deep inelastic processes but, in addition, fusion-evaporation reactions with the ^{16}O target contaminant leads to the population of ^{89}Rb. In the experiment of Pawlat *et al.* [61], neutron-rich ^{89,91}Rb nuclei were populated as fission products in heavy-ion reactions and decay γ rays were detected using the GAMMASPHERE Ge multi-detector array. In the work of Bucurescu *et al.* [3], states were observed up to an excitation energy of 4033 keV and the highest spin assignment was (19/2, 21/2) whereas, in the work of Pawlat *et al.*, the level structure was extended up to an excita-

tion energy of 7391 keV and the highest spin assignment was $(25/2^+)$ (E_x = 5606 keV). In the most recent work of Astier *et al.* [60], high-spin states of ^{88}Kr and of ^{89}Rb were studied using the ^{18}O + ^{208}Pb fusion-fission reaction. Gamma rays emitted from the fission fragments were detected with the EUROBALL array of escape-suppressed Ge γ-ray detectors at the IReS Strasbourg Laboratory. States of ^{89}Rb were studied to an excitation energy of 7389 keV ($J^\pi = (29/2^+)$), with the order of the 686 and 1098 keV transitions at the top of the previously established high-spin decay sequence inverted. In addition, a few new transitions were observed, both in the high-spin and low-spin parts of the level scheme. Gamma-ray angular correlation measurements for the most intense γ-ray transitions were used to determine the dipole or quadrupole nature of transitions. The level structure of ^{89}Rb was earlier studied using β decay [62] and in the ^{86}Kr(α, p) reaction [54]. In the latter work, J assignments up to 11/2 were proposed. The level scheme of fig. 4, corresponding to previously published work, is based on the publications of Astier *et al.* [60], Bucurescu *et al.* [3], and Pawlat *et al.* [61] and the J^π values of Astier *et al.* [60] are those that are given. There is a disagreement between the work of Astier *et al.* [60] and those of Bucurescu *et al.* [3] and Pawlat *et al.* [61] in relation to the J^π assignment for the state at E_x = 586 keV; the latter publications have assigned a J^π value of (7/2), whereas Astier *et al.* [60] have assigned $5/2^-$. It is noted that the evaluation of Singh [54], which does not include the publication of Astier, has a spin assignment of $7/2(^-)$ for the state.

Figure 5 presents γ-ray spectra corresponding to two different reaction Total Kinetic Energy Loss (TKEL) values [63], measured in coincidence with residual nuclei of ^{89}Rb detected and identified at the focal plane of PRISMA. In the γ-ray spectrum of fig. 5(a), the 809, 836, 1193, and 1572 keV transitions show an enhancement in yield relative to the other transitions compared with the same transitions in the spectrum of fig. 5(b), indicating that they are emitted from higher-lying states (with higher TKEL values). From fig. 5 it is possible, for example, to deduce that the 836 keV γ ray is emitted from a state lying higher in energy than is the case for the 809 keV γ ray. Figure 6 presents two examples of double-gated γ-ray spectra from the GASP experiment. The upper spectrum, fig. 6(a), corresponds to the first gate set on the 809 keV photopeak, in coincidence with gates set on the 198 keV and 264 keV photopeaks. The lower spectrum, fig. 6(b), corresponds to the first gate set on the 836 keV transition in coincidence with the 1193 keV transition. The analysis of such spectra forms the basis for establishing coincidence relationships between transitions of ^{89}Rb. The identification of ^{89}Rb γ rays in the PRISMA/CLARA experiment, in combination with the coincidence data from the GASP experiment, allows us to construct the level scheme presented in fig. 4. Measured asymmetry ratios (table 3) and γ-γ angular correlation measurements (table 4) have resulted in proposed multipolarity assignments (see column 5 of table 3).

The E_x = 1195 keV isomeric state was assigned a J^π value of $9/2^+$ by Astier *et al.* [60] and a lifetime of a few nanoseconds by Bucurescu *et al.* The lifetime is consistent with an $M2$ multipolarity for the $9/2^+ \rightarrow 5/2^-$ 974 keV transition. In the more recent work of Pawlat *et al.* [61], the half-life was measured to be 8(2) ns. In the present work, see fig. 5, the 975 keV transition is not seen in the PRISMA/CLARA experiment, which indicates that most of the γ-ray decay occurs outside the CLARA reaction chamber; consequently, it can be concluded that the half-life is longer than circa 6 ns. A more precise half-life measurement has been made here for the state using data from the GASP experiment (A preliminary report on the measurement was given in ref. [64]). Briefly, in fig. 7 a Ge-time signal *versus* E_γ matrix is shown. In the creation of the matrix, only γ rays in coincidence with the 221 keV, $5/2^- \rightarrow 3/2^-$, transition and any of the γ rays of energy 809 keV ($13/2^+ \rightarrow 9/2^+$), 836 keV ($17/2^+ \rightarrow 13/2^+$), and 1193 keV ($21/2^+ \rightarrow 17/2^+$) were included. From fig. 7 it is clear that the 975 keV transition is isomeric. The presence of known isomers in the data ($T_{1/2}$ = 103(3) ns in ^{97}Zr and $T_{1/2}$ = 6(1) ns in ^{87}Rb) allowed an internal calibration [64,65] of the time scale to be made. The measured half-life of 15(3) ns is not in good agreement with the value of Pawlat *et al.* [61] ($T_{1/2}$ = 8(2) ns). It is consis-

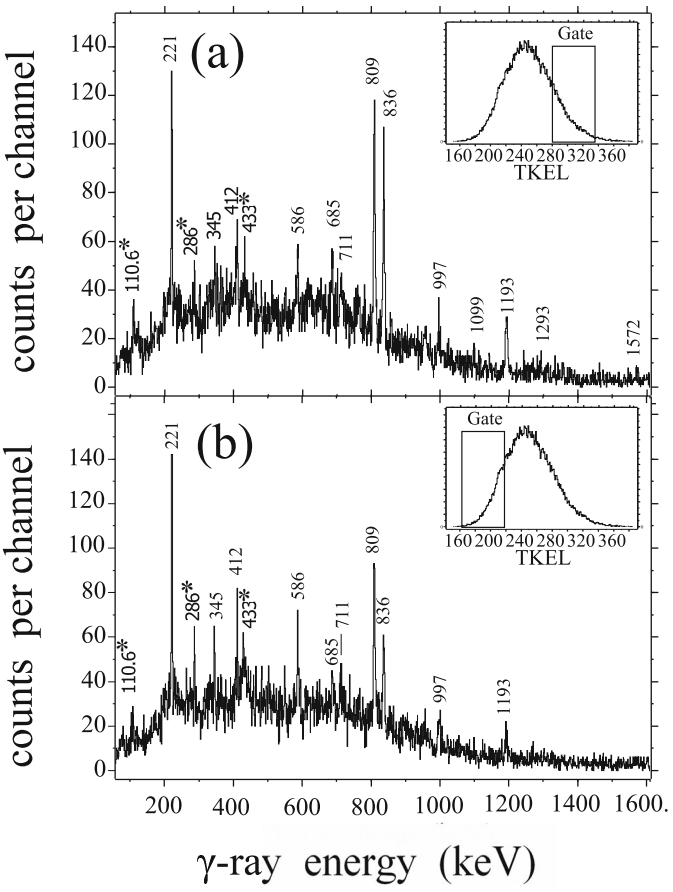

Fig. 5. Gamma-ray energy spectra measured in coincidence with the A = 89 mass for Z = 37 (^{89}Rb) and corresponding to high (upper panel) and low (lower panel) TKEL values (arbitrary units) for the PRISMA/CLARA experiment. Gamma-ray photopeaks marked with an asterisk correspond to transitions which belong to ^{89}Rb but with no assigned position in the level scheme. See text for details.

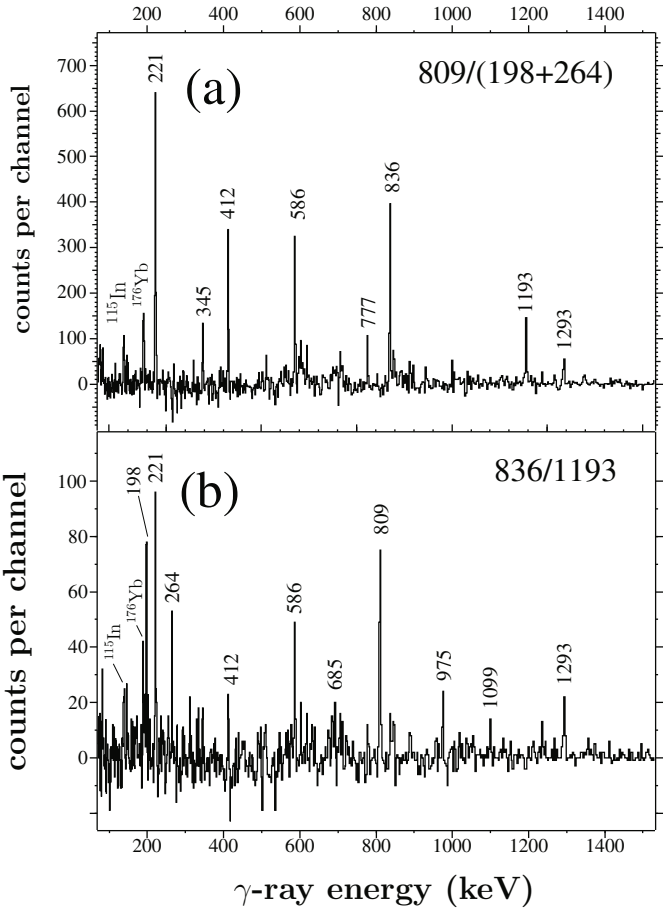

Fig. 6. Double-gated γ-ray energy spectra for ^{89}Rb from the GASP experiment. See text for details.

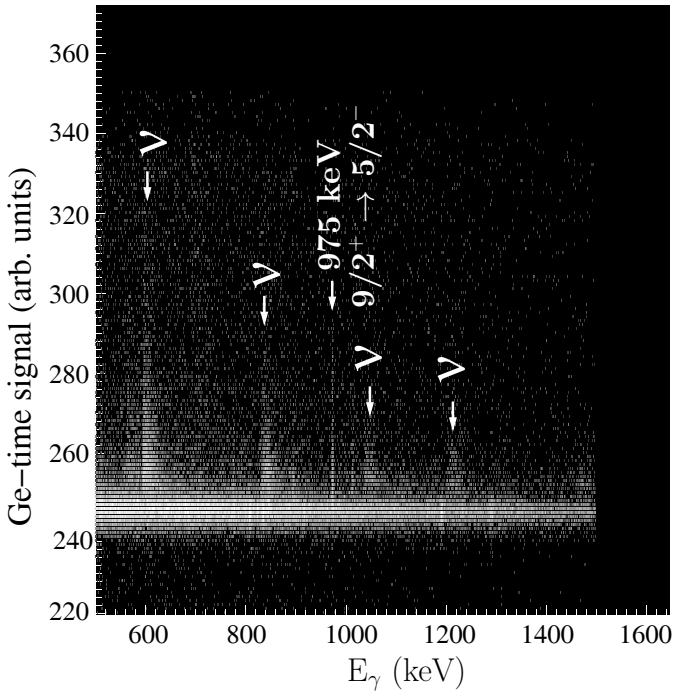

Fig. 7. Two dimensional spectrum of Ge-time signal (y axis) *versus* γ-ray energy (x axis). The 975 keV line corresponds to γ-ray emission from the $9/2^+$ state in ^{89}Rb. Neutron peaks are labelled with the symbol ν. See text for details.

tent with the $M2$ character of the 975 keV decay; the hindrance, when compared to the Weisskopf estimate, is 8.5, a value in very good agreement with the hindered $M2$ decay (hindrance = 8.6) of the isomeric $9/2^+$ state of ^{87}Rb, discussed earlier. In the present work, we have identified for the first time a very weak γ-ray branch ($E_\gamma = 1195$ keV) from the isomeric state to the ground state, presumably of $E3$ multipolarity. This branch was also observed, it will be recalled, in ^{87}Rb.

The level scheme above the $J^\pi = 9/2^+$ isomeric state, based on the present experiments, agrees well with the most recent published work, that of Astier *et al.* [60], see fig. 4. A 1267 keV transition, connecting the $(23/2^-)$ state to the $21/2^+$ state, was observed by Astier *et al.* [60], but was not identified in the present work or in those of Pawlat *et al.* [61] and Bucurescu *et al.* [3]. A 1372 keV transition which connects states at $E_x = 6700$ keV ($J^\pi = (29/2^+)$) and 5328 keV ($J^\pi = (25/2^+)$) was observed by Astier *et al.* and by Bucurescu *et al.*, but remains unobserved here. In addition, a 913 keV transition from a previously unidentified 3752 keV state ($J^\pi = (21/2^+)$) to the $17/2^+$ state at $E_x = 2841$ keV has been observed only by Astier *et al.* [60].

The transitions above the $9/2^+$ state, with $E_\gamma = 809$, 836, 1193, and 1572 keV, have a quadrupole character confirmed by the asymmetry ratios (table 3) and the γ-γ angular correlation measurements (table 4). On the basis that the sequence of four transitions is of $E2$, rather than $M2$ character, we assign J^π values of $13/2^+$, $17/2^+$, $21/2^+$, and $25/2^+$ to the states of excitation energy 2005, 2841, 4033, and 5605 keV, respectively. For the 809 and 836 keV transitions, for example, the predicted half-lives (assuming a hindrance factor of 10) for $M2$ transitions are 45 ns and 38 ns, respectively, which excludes the possibility of the transitions being of $M2$ multipolarity. The same spin-parity assignments were made to the first three states of this sequence by Pawlat *et al.* [61], again based on the results of a γ-ray angular correlation analysis. Astier *et al.* [60], on the basis of a measurement of the angular-correlation of successive γ rays, assigned a quadrupole multipole order to three of the transitions, but the 1572 keV transition remained unassigned. In the work of Bucurescu *et al.* [3], the experimental γ-ray angular distribution data were unable to yield a definitive multipolarity assignment for the 1193 keV transition, although the 809 and 836 keV transitions were unambiguously assigned as quadrupole. The 686 keV transition has previously been observed by Pawlat *et al.* and, more recently, by Astier *et al.*, but no multipolarity assignment was made. From its measured R_{asym} value of 0.63(17) (see table 3), a dipole character can be assigned to the transition, leading to a proposed $(27/2^+)$ spin assignment for the 6291 keV state. The highest state reported at $E_x = 7390$ keV deexcites through the emission of a 1099 keV γ ray. Here, the placement of the 686 and

1099 keV γ-ray transitions in the level scheme agrees with the work of Astier *et al.* [60], but not with that of Pawlat *et al.* [61]. However, the evidence for this placement, based on measured γ-ray intensities, is much more convincing in the present work than in that of Astier *et al.*, where the two intensities are the same, within the quoted experimental errors. The multipolarity of the 1099 keV transition is currently unknown; Astier *et al.* [60] have proposed a J^π value of $(29/2^+)$ for the 7390 keV state; this does not appear to be supported by experimental measurement. From the PRISMA/CLARA setup it is possible to observe γ rays at energies of 111, 286, and 433 keV; these three transitions belong to the ^{89}Rb nucleus, but they could not be placed in the level scheme. In the recent evaluation of Singh [54], they are not listed in the previously observed ^{89}Rb γ-ray transitions.

For the 586 keV transition, the observed quadrupole nature (see tables 3 and 4), together with the predicted long half-life for an $M2$ transition (assuming a hindrance factor of 10), namely 230 ns, indicates an $E2$ multipolarity for this transition. On this basis, it is proposed that the J^π value of the state at $E_x = 586$ keV is $7/2^-$. This is in disagreement with the $5/2^-$ spin assignment for the state made by Astier *et al.* [60].

In sect. 4, the structure of ^{89}Rb will be discussed in the context of the shell model.

3.3 ^{91}Rb experimental results

States of ^{91}Rb with spin values up to 7/2 were previously studied [69,70] using β^--γ coincidences from the decay of ^{91}Kr. More recently, fusion-fission and multinucleon transfer reactions were used to populate medium to high-spin states. In the work of Pawlat *et al.* [61], referred to above in the discussion of ^{89}Rb, states of ^{91}Rb were populated up to an excitation energy of 6239 keV and J^π assignments were proposed, based on γ-γ angular correlation measurements, for excited states up to 4097 keV ($J^\pi = 21/2^+$). The spontaneous fission of ^{252}Cf was used by Hwang *et al.* [66] in a study of ^{91,92,93}Rb; in this work, states of ^{91}Rb were observed up to an excitation energy of 4097 keV with the γ-ray decay studied using the GAMMASPHERE array. The spins of positive-parity states of ^{91}Rb were assigned from a comparison with those of ^{89}Rb. The most recent study of medium-spin states of ^{91,93,95}Rb was made by Simpson *et al.* [67]; states of ^{91}Rb were populated using the spontaneous fission of ^{248}Cm and ^{252}Cf sources and levels with excitation energy up to 5298 keV were studied. In the work of Simpson *et al.* [67], no γ-ray angular correlation data could be collected for the observed transitions of ^{91}Rb because of the low population of ^{91}Rb and contaminating transitions from other nuclei. The most recent evaluation of experimental nuclear structure and decay data for all known $A = 91$ nuclides was published by Baglin [68] in 2013. The J^π values of states from previous studies presented in fig. 8 were taken from the published level scheme of Pawlat *et al.* [61], with the exception of the 722 keV state, where the J^π value is that of Hwang *et al.* [66]. For the $9/2^+$ isomeric state and the decay sequence built on it, the J^π assignments made by Hwang *et al.* agree with those of Pawlat *et al.*, but the former work places the J^π assignments in parentheses. The excitation energies of states, corresponding to previous work in fig. 8, were taken from the work of Simpson *et al.* [67]. The excitation energy of the state at 6239 keV, unobserved by Simpson, was taken from Pawlat *et al.* [61].

In fig. 9, the γ-ray energy spectrum in coincidence with mass $A = 91$ and $Z = 37$ from the PRISMA/CLARA experiment is shown. The peak to background ratio is inferior to that of the γ-ray spectra presented earlier for the ^{87,89}Rb isotopes. The level scheme of fig. 8, corresponding to the present work, is informed by earlier work, and is based on the relative intensities of transitions in the γ-ray energy spectra corresponding to different values of TKEL, on γ-ray intensity balance, and, importantly, on the results of an analysis of ^{91}Rb triples coincidences from the GASP experiment. Table 5 presents the energies (E_i) of excited states in ^{91}Rb together with transition energies (E_γ), relative γ-ray intensities (I_γ) (based on the GASP experiment), and γ-ray asymmetry ratios (R_{asym}). Proposed multipolarities, informed by previous work and based on the present work, appear in column five of table 5, followed by the proposed spins and parities of the initial and final states. The final two columns present the J^π and multipolarity assignments from the 2013 Nuclear Data Sheets evaluation [68]. Quantities in italics correspond to new level energies or previously unobserved γ-ray transitions. Figure 10 presents an example of a double-gated γ-ray spectrum from the GASP experiment in which the first gate is set on the 706, 1138, and 474 keV photopeaks and the second gate is set on the 412 keV photopeak. The intensities of the γ-ray transitions at energies of 474, 1119, and 728 keV are, within the experimental errors, the same. Consequently, in the present work, we are unable to establish the order of the transitions within the ^{91}Rb level scheme. Otherwise, the present level scheme agrees with the results of the earlier work of Pawlat *et al.* [61], Hwang *et al.* [66], and Simpson *et al.* [67]. The 502 keV level, previously observed in the beta decay of ^{91}Kr [69,70], was also populated here and, in addition, new levels are tentatively proposed at $E_x = 993$ keV and at 2167 keV. It is noted that the 502 keV level was not observed in the published work of Pawlat *et al.* [61], Hwang *et al.* [66], and Simpson *et al.* [67].

The transitions of energy 502 and 993 keV, which directly populate the ground state, have asymmetry ratios (see table 5) which are consistent with quadrupole multipolarity. An $M2$ assignment is excluded as a consequence of the long half lives for $M2$ transitions (480 and 16 ns, respectively, with an assumed hindrance factor of 10). Consequently, a J^π value of $(7/2^-)$ is assigned to each decaying state, at excitation energies of 501.8 and 993.1 keV. A hitherto unobserved [68] 505.3(2) keV transition, with an asymmetry ratio (see table 5) consistent with quadrupole multipolarity remains unplaced in the level scheme. The 505 keV photopeak appears in the γ-ray spectrum measured in coincidence with ^{91}Rb ions detected at the focal plane of PRISMA, fig. 9, and this ob-

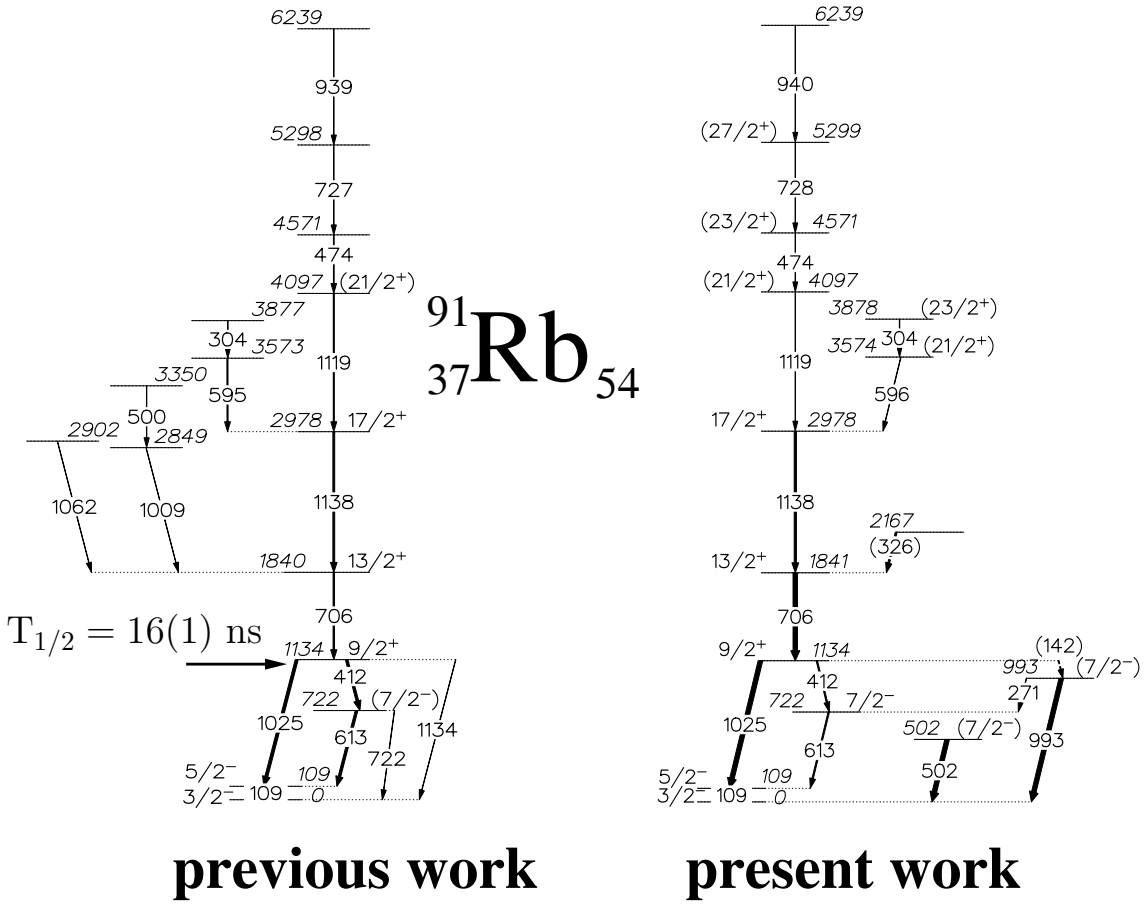

Fig. 8. Proposed level scheme of ^{91}Rb. The level scheme corresponding to earlier work is based on refs. [61,66,67]. Energies are in units of keV, given to the nearest integer value, and the widths of arrows are proportional to the relative intensities of the γ-ray transitions. Measured γ-ray energies are presented in table 5. See text for details.

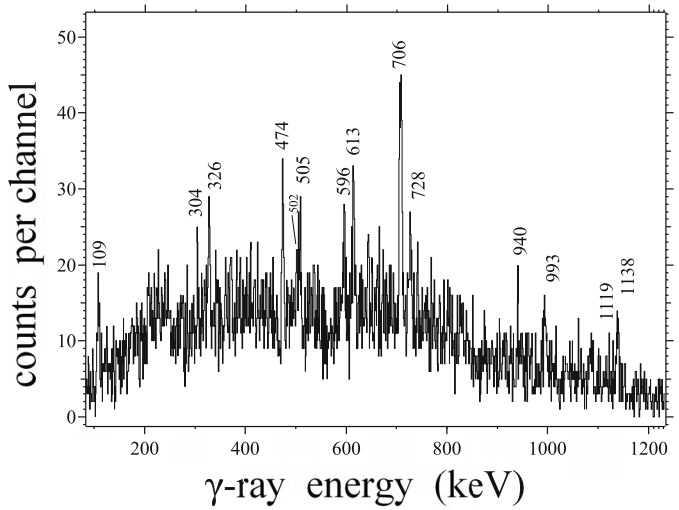

Fig. 9. Gamma-ray energy spectrum in coincidence with the $A = 91$ mass for $Z = 37$ (^{91}Rb) identified at the focal plane of PRISMA.

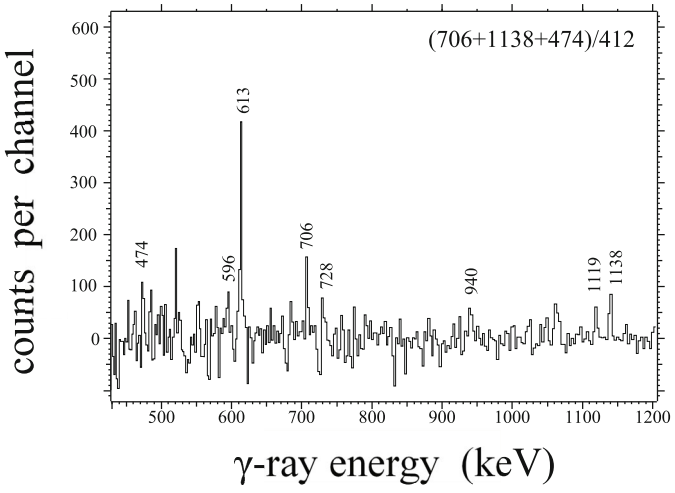

Fig. 10. Double-gated γ-ray spectrum for ^{91}Rb from the GASP experiment.

servation excludes a multipolarity of $M2$ for the transition (470 ns lifetime, assuming a hindrance factor of 10).

The 993 keV state has not previously been observed; the 271 and 993 keV γ rays which deexcite the state have not previously been attributed to ^{91}Rb [68]. The γ-ray photopeak at an energy of 1025 keV, corresponding to the

Table 5. The energies (E_i) of excited states of ^{91}Rb, together with transition energies (E_γ), relative γ-ray intensities (E_γ) (based on the GASP experiment), and γ-ray asymmetry ratios (R_{asym}). Proposed multipolarities, based on the present work, appear in column five of the table, followed by the proposed spins and parities of the initial and final states. The final two columns present the J^π and multipolarity assignments from the 2013 Nuclear Data Sheets evaluation [68]. Quantities in italics correspond to new level energies or previously unobserved γ-ray transitions.

E_i (keV)	E_γ (keV)	I_γ	R_{asym}	Proposed mult.	J_i^π	$\rightarrow$	J_f^π	J^π [68]	Multipolarity [68]
108.91(19)	108.90(20)	40(5)	0.50(12)	$M1/E2$	$5/2^-$	$\rightarrow$	$3/2^-$	$(5/2^-)$	$M1(+E2)$
501.80(20)	501.80(20)	18(3)	1.65(48)	$E2$	$(7/2^-)$	$\rightarrow$	$3/2^-$		
722.0(3)	613.10(20)	30(8)	0.83(24)	$M1/E2$	$7/2^-$	$\rightarrow$	$5/2^-$	$(\leq 7/2^-)$	$(M1, E2)$
993.1(4)	*271.2(10)*	< 1			$(7/2^-)$	$\rightarrow$	$7/2^-$		
	993.1(4)	25(5)	1.26(40)	$E2$	$(7/2^-)$	$\rightarrow$	$3/2^-$		
1134.2(3)	141.5(10)	< 1			$9/2^+$	$\rightarrow$	$7/2^-$	$(9/2^+)$	
	412.20(20)	5(2)			$9/2^+$	$\rightarrow$	$7/2^-$		
	1025.3(3)	10(3)		$M2$	$9/2^+$	$\rightarrow$	$5/2^-$		$(M2)$
1840.7(3)	706.50(20)	100(12)	1.22(29)	$E2$	$13/2^+$	$\rightarrow$	$9/2^+$	$(13/2^+)$	quadrupole
2166.7(11)	*326.0(10)*	12(3)				$\rightarrow$	$13/2^+$		
2978.3(5)	1137.6(4)	50(7)	1.15(29)	$E2$	$17/2^+$	$\rightarrow$	$13/2^+$	$(17/2^+)$	quadrupole
3573.9(7)	595.6(4)	35(5)			$(21/2^+)$	$\rightarrow$	$(17/2^+)$		
3878.4(21)	304.5(20)	11(3)			$(23/2^+)$	$\rightarrow$	$(21/2^+)$		
4097.4(6)	1119.1(3)	20(5)	1.29(49)	$E2$	$(21/2^+)$	$\rightarrow$	$(17/2^+)$	$(21/2^+)$	quadrupole
4571.2(12)	473.8(10)	22(5)	0.50(34)	$M1/E2$	$(23/2^+)$	$\rightarrow$	$(21/2^+)$		
5298.8(13)	727.6(5)	20(5)	1.13(40)	$E2$	$(27/2^+)$	$\rightarrow$	$(23/2^+)$		
6239.0(13)	940.2(4)	17(4)							
	505.30(20)	24(4)	1.41(50)	$E2$					

depopulation of the $J^\pi = 9/2^+$ state at 1134 keV, can be seen in the thick target GASP experiment, but not in the PRISMA/CLARA experiment; this observation is consistent with the known isomerism of the state [69,67]. Previous measurements of half-lives have yielded values of 17.0(8) ns [69] and 16(1) ns [67]. For transitions above the $9/2^+$ isomeric state, the asymmetry ratios allow an assignment of multipolarity for the γ rays at energies of 706, 1138, 1119, 474, and 728 keV. With the exception of the 474 keV, $(23/2^+) \rightarrow (21/2^+)$ transition, for which a mixed $M1/E2$ character is assigned, the asymmetry ratios are consistent with quadrupole multipolarity. $M2$ transitions, with an assumed hindrance factor of 10, for these quadrupole transitions, have half lives in the range from 8 to 90 ns and, on this basis, we propose here $E2$ assignments. The tentative J^π values for the 4097, 4571, and 5299 keV states, shown in fig. 8, are based on these multipolarity assignments.

4 Shell-model calculations

Spherical shell-model calculations have been performed in order to understand the microscopic structure of the odd-A Rb isotopes studied here. The set of codes CENS (Computational Environment for Nuclear Structure) from Oslo University was utilized [72] in the calculations. An effective two-body interaction was derived microscopically from the Idaho N3LO nucleon-nucleon potential [73] using a $V_{\text{low-}k}$ renormalization procedure [74]. A model space outside a $^{78}_{28}\text{Ni}_{50}$ core was used, with single-particle states $\pi(1f_{5/2}, 2p_{3/2}, 2p_{1/2}, 1g_{9/2})$ and $\nu(2d_{5/2}, 2d_{3/2}, 3s_{1/2}, 1g_{7/2})$. Promotion of neutrons across the $N = 50$ shell gap is not allowed in these calculations. The available single-particle energies (SPE) used in the calculations were taken from ref. [71]. Those SPE not available in the literature were calculated in the Hartree-Fock approximation using the Skyrme SLy4 parameterization [75]. A modification of 10% in the value of the SPE for the $1g_{9/2}$ orbital, from -9.08 MeV [71] to -10.08 MeV, was introduced to reproduce the position of the $9/2^+$ isomeric level. The values of SPE are shown in table 6. Within the context of the simple shell model, the isotopes of Rb with $A = 87$, 89, and 91 have, in their ground states, a proton configuration of $(1f_{5/2})^6(2p_{3/2})^3(2p_{1/2})^0(1g_{9/2})^0$ and neutron configurations of $(1g_{9/2})^{10}(2d_{5/2})^{(N-50)}(2d_{3/2})^0(3s_{1/2})^0(1g_{7/2})^0$, where $N = 50$, 52, and 54 for ^{87}Rb, ^{89}Rb, and ^{91}Rb, respectively. The calculations which will now be discussed below show that this is a reasonably good approximation to the shell-model description of the ground-state configurations. To make the calculations possible, it was neces-

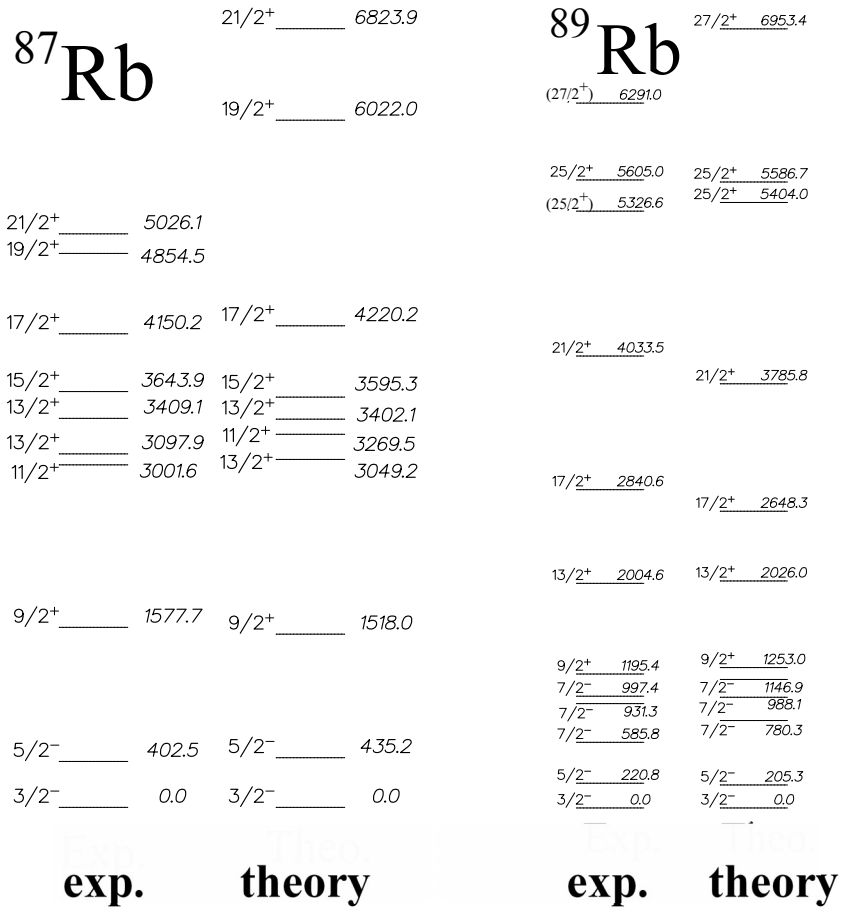

Fig. 11. The results of shell-model calculations for ^{87}Rb and ^{89}Rb. Partial experimental level schemes are presented for comparison. Excitation energies are in units of keV.

sary to make a truncation of the occupation numbers. At most, three protons were allowed to occupy the $2p_{1/2}$ and $1g_{9/2}$ orbitals. The results of the shell-model calculations for ^{87}Rb and ^{89}Rb are presented in fig. 11. Figures 12 and 13 present the shell-model nucleon orbit occupations for the positive-parity states built on the $J^\pi = 9/2^+$ isomeric state for ^{87}Rb and ^{89}Rb, respectively. For these states, the figures also present the difference between the shell-model excitation energies and the experimental values. There are two $13/2^+$ states predicted and two observed in ^{87}Rb and both states are included in fig. 12. A horizontal bar has been drawn through the data points corresponding to the $13/2^+$ yrast state, which does not form part of the strong decay sequence built on the $9/2^+$ isomeric state. Similarly, there are two predicted and observed states of ^{89}Rb with $J^\pi = 25/2^+$ and, in fig. 13, the data points corresponding to the state of lower excitation energy are indicated by a horizontal bar.

For ^{87}Rb and ^{89}Rb, the $3/2^-$ ground states are expected to correspond to a proton hole in the $2p_{3/2}$ shell, while the first excited $5/2^-$ states are expected to correspond to a vacancy in the $1f_{5/2}$ proton shell, *i.e.* $\pi(1f_{5/2})^5 (2p_{3/2})^4$. The results of the shell-model calculations performed here are in good agreement with these simple shell-model orbit occupations; for the $3/2^-$ states of ^{87}Rb and ^{89}Rb, the shell-model occupations are 5.8 and 5.7, respectively for the proton $1f_{5/2}$ orbital and 2.9 and 2.8, respectively, for the proton $2p_{3/2}$ orbital. For the $5/2^-$ state, the corresponding proton occupancies are 5.0 and 5.9 for the $1f_{7/2}$ orbital and 3.7 and 3.7 for the $2p_{3/2}$ orbital. Within the uncertainties associated with the DWBA analysis of single-nucleon transfer reactions (principally associated with the description of the entrance and exit channels using optical-model potentials and the parameterisation of the Woods-Saxon bound-state potential), the conclusions from published proton stripping [43] and pickup [44] reactions are broadly in agreement with such descriptions of

Table 6. Single-particle energies with respect to a ^{78}Ni core. Values are from ref. [71] except for those values with an asterisk which were calculated using a Skyrme interaction.

nlj	ϵ^π_{nlj} ^{87,89}Rb	ϵ^π_{nlj} (MeV) ^{91}Rb	nlj	ϵ^ν_{nlj} (MeV) ^{87,89,91}Rb
$1f_{5/2}$	−15.11	−16.10	$1g_{7/2}$	3.04*
$2p_{3/2}$	−13.42		$2d_{5/2}$	−2.41
$2p_{1/2}$	−12.23		$2d_{3/2}$	0.99*
$1g_{9/2}$	−10.08	−12.08	$3s_{1/2}$	0.27*

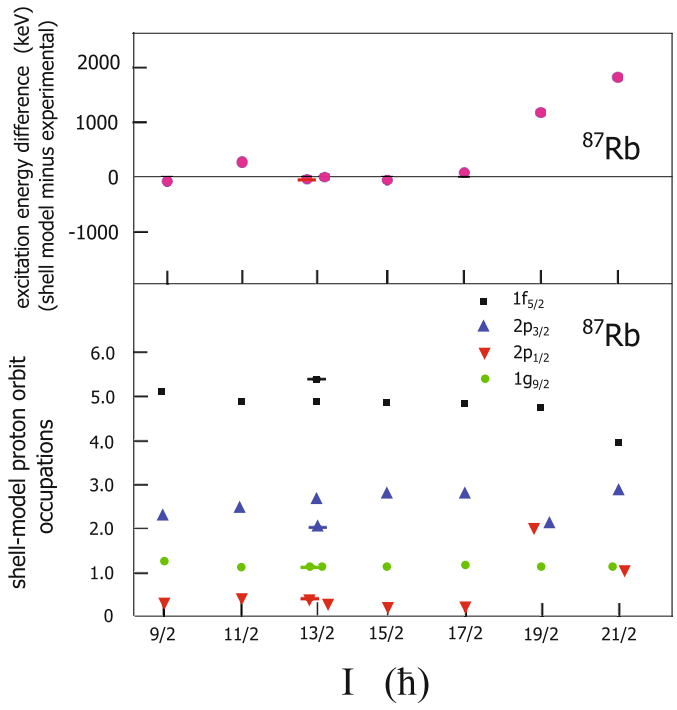

Fig. 12. The results of shell-model calculations for ^{87}Rb for states with $I \geq 9/2$. The upper panel shows the difference between shell-model and experimental excitation energies for the positive parity sequence of states, while the lower panel shows the shell-model proton orbit occupations. See text for details.

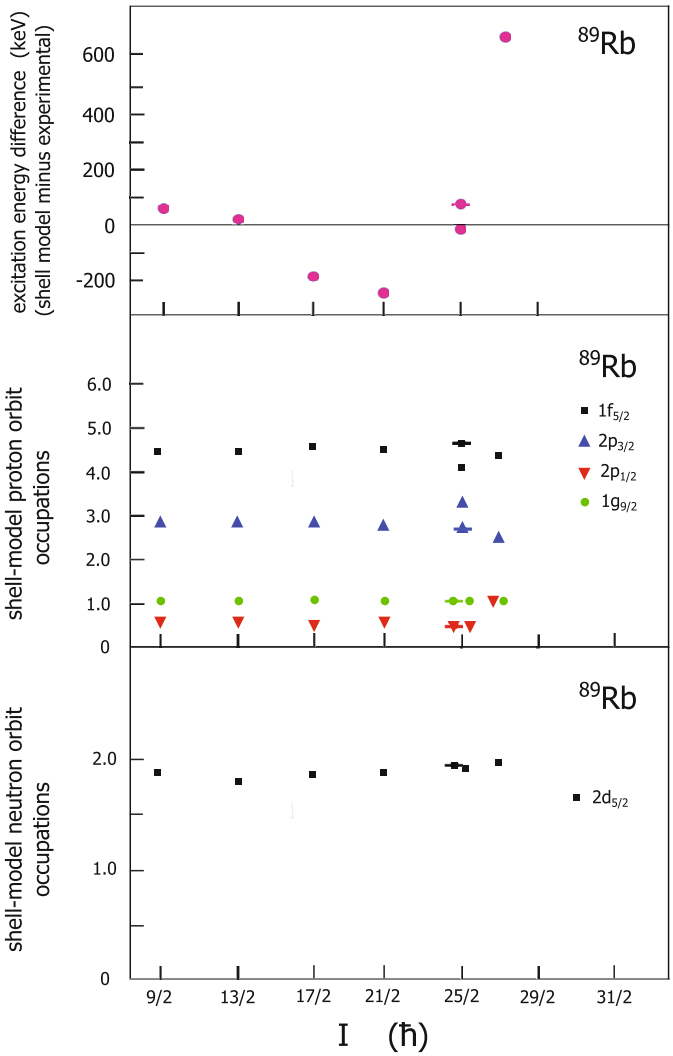

Fig. 13. The results of shell-model calculations for ^{89}Rb for states with $I \geq 9/2$. The upper panel shows the difference between shell model and experimental excitation energies for the positive parity sequence of states, while the lower panels show the shell-model proton and neutron orbit occupations. See text for details.

the ground state of ^{87}Rb and the excited state at $E_x = 402\,\mathrm{keV}$ with $J^\pi = 5/2^-$. In addition, as noted earlier, the published proton stripping reaction $^{86}\mathrm{Kr}(^3\mathrm{He}, \mathrm{d})^{87}\mathrm{Rb}$ populates the 1578 keV $9/2^+$ state with a spectroscopic strength of $(2J+1)S = 9.9$ [43], which is consistent with the description of the state as a pure $1g_{9/2}$ proton excitation. The $9/2^+$ state of ^{89}Rb at $E_x = 1195\,\mathrm{keV}$ was strongly populated in the $^{86}\mathrm{Kr}(\alpha, \mathrm{p})^{89}\mathrm{Rb}$ reaction in an $L = 4$ transfer with $\sigma(\mathrm{exp})/\sigma(\mathrm{DWBA}) = 4.3$ [54]. Presumably, the three-nucleon transfer process involves the transfer of a neutron pair into the $2d_{5/2}$ orbital, coupled to spin zero, and the transfer of a proton into the $1g_{9/2}$ orbital. For ^{87}Rb, ^{89}Rb, and ^{91}Rb, the low-lying negative parity states correspond to occupation of the $1f_{5/2}$, $2p_{3/2}$ and $2p_{1/2}$ proton orbitals, with the $1g_{9/2}$ proton shell essentially empty.

The positive-parity decay sequences in ^{87}Rb, ^{89}Rb, and ^{91}Rb are built on the $J^\pi = 9/2^+$ isomeric state for which the $1g_{9/2}$ orbit is occupied by one proton; within the shell-model configuration space, this is the only way in which positive-parity states can be formed. For ^{87}Rb, the positive-parity sequence up to the $17/2^+$ state is very well reproduced in the calculations (see figs. 11 and 12). This implies that these high-spin states are well described within the context of the shell model in terms of a single proton in the $1g_{9/2}$ orbital coupled to excitations of the proton core, with neutrons occupying the lowest available shell-model orbitals. For the $J^\pi = 19/2^+$ and $21/2^+$ states, there is a significant disagreement between the shell-model and experimental excitation energies, and this is probably related to the restricted configuration space of the present shell-model calculations. Presumably, a more satisfactory shell-model description of these states involves promotion of a neutron into the available orbits beyond the $N = 50$ shell gap. This has been discussed in an earlier publication [22]. For ^{89}Rb, the overall agreement between experiment and shell model is reasonably good for positive parity states up to $25/2^+$; in this case neutrons are allowed to occupy the whole of the sdg shell. The excitation energy of the $J^\pi = 29/2^+$ state is not well reproduced; the difference between experimental and shell-model excitation energies is about 660 keV.

Figure 14 presents a comparison of the shell-model results for ^{91}Rb and experiment. It is again noted that the experimental J^π values in parentheses are specula-

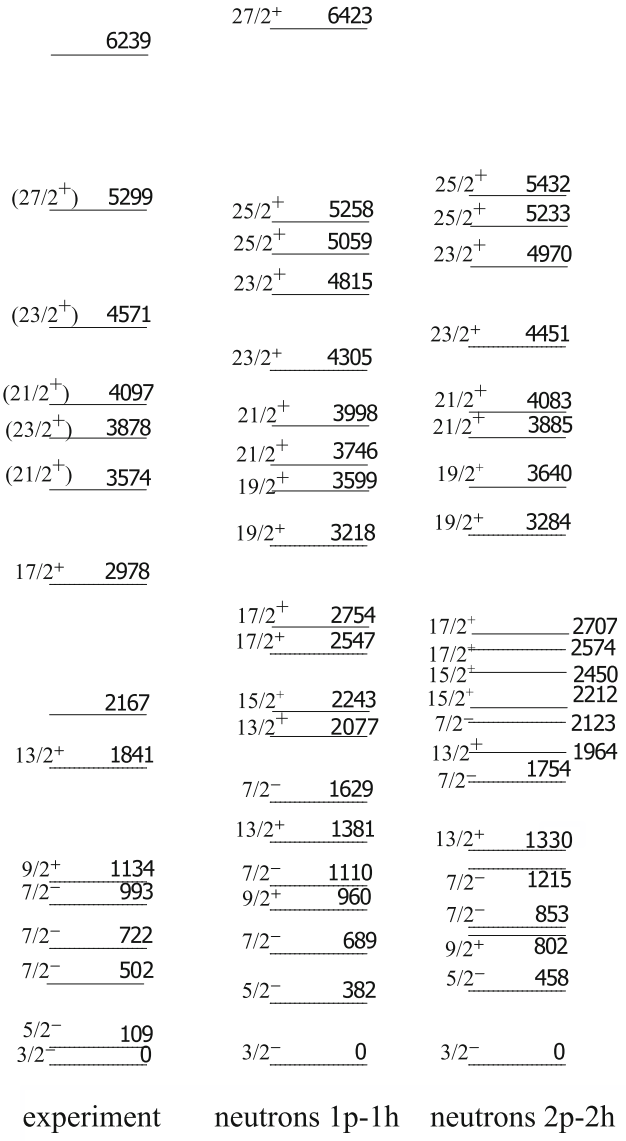

Fig. 14. The results of shell-model calculations for ^{91}Rb. The experimental level scheme based on the present work is presented for comparison. Excitation energies are in units of keV. See text for details.

tive. Since the main focus of interest here is related to the higher-spin states of ^{91}Rb, in fig. 14 the first two shell-model states of a given J^π value are included for states with $J^\pi \geq 13/2^+$. The results of two calculations, corresponding to neutron one-particle one-hole configurations and two-particle two-hole configurations are presented in the figure. In the neutron one-particle one-hole calculation, only one state with $J^\pi = 15/2^+$ was predicted. Unlike the situation in ^{87}Rb and in ^{89}Rb, the first excited $J^\pi = 5/2^-$ state of ^{91}Rb, observed experimentally at 109 keV, is not well reproduced in the shell-model calculation. Similarly, the excitation energy of the $9/2^+$ bandhead of the positive-parity decay sequence is not well reproduced, in contrast to ^{87}Rb and ^{89}Rb. It is possible, for each experimental state above the $9/2^+$ isomer, to identify

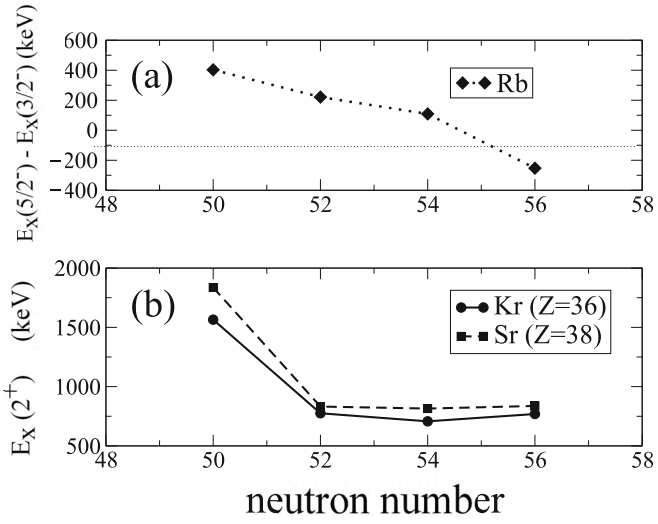

Fig. 15. Upper figure, (a) energy difference between the $5/2^-$ and $3/2^-$ states for the odd-A Rb isotopes. Lower figure (b), $E_x(2_1^+)$ as a function of neutron number for the Kr and Sr isotopes. See text for details.

an association of experimental and shell-model states but, given the number of relatively close lying high-spin shell-model states and the uncertainties in the experimental J^π values, the confidence in doing so is considerably reduced compared to the association for ^{87}Rb and ^{89}Rb. For the experimental states at 1134 keV, 1841 keV, and 2978 keV, the J^π values have been established as $9/2^+$, $13/2^+$, and $17/2^+$, respectively. The corresponding shell-model states are those at excitation energies of 960, 1381, and 2547 keV, respectively, for the neutron one-particle one-hole calculation and 802, 1330, and 2574 keV for the neutron two-particle two-hole calculation. The state observed in the present work at an excitation energy of 2167 keV has no assigned J^π value; it is expected to be an yrast or near yrast state. On this basis, it is speculated that the associated shell-model state is either that at 2077 keV with $J^\pi = 13/2^+$ or that at 2243 keV with $J^\pi = 15/2^+$.

With neutron numbers in the range from 52 to 56, neutrons gradually fill the $2d_{5/2}$ shell-model state. There will be a strong neutron-proton attractive tensor interaction [76] between the $j_>2d_{5/2}$ neutrons and the $j_<1f_{5/2}$ protons which will lead to an increased binding of the $5/2^-$ state. Figure 15(a) shows the evolution of the excitation energy difference between the $5/2^-$ state and the $3/2^-$ ground state for the Rb isotopes with $N = 50$, 52, 54, and 56. The decrease in $E_x(5/2^-) - E_x(3/2^-)$ with increasing neutron number would appear to be consistent with the expected effects of the tensor interaction. It is also possible that the $J^\pi = 5/2^-$ states have components in their wave function corresponding to the coupling of a $2p_{3/2}$ proton to the $J^\pi = 2_1^+$ state of the core and this could potentially provide an explanation for the observed behaviour shown in fig. 15(a). However, a comparison of the observed energy trends in fig. 15(a) and fig. 15(b) leads to the conclusion that this explanation is incorrect. It is noted here that, while the shell-model results presented earlier are able to reproduce the energy difference between

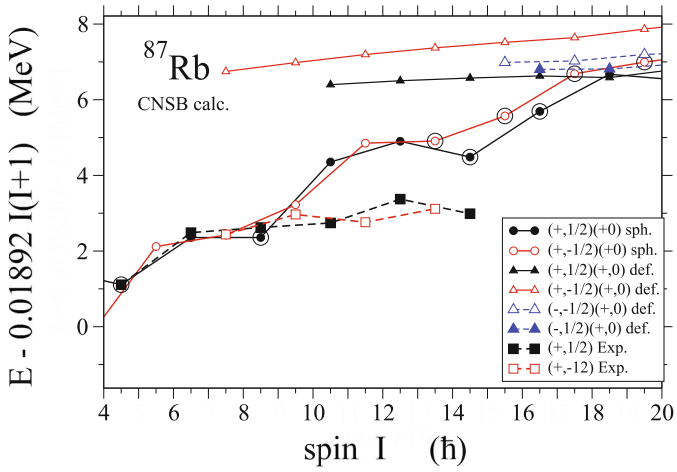

Fig. 16. Energies for selected configurations of $^{87}_{37}\mathrm{Rb}_{50}$ calculated in the CNSB formalism and labelled by the proton and neutron parity and signature, $(\pi,\alpha)_p(\pi,\alpha)_n$. Energies are given relative to an 0.01892 $I(I+1)$ reference. Experimental values assigned to $\pi = +$ are drawn with squares. A normalization to the $I^\pi = 9/2^+$ state is used when comparing experimental data with calculations.

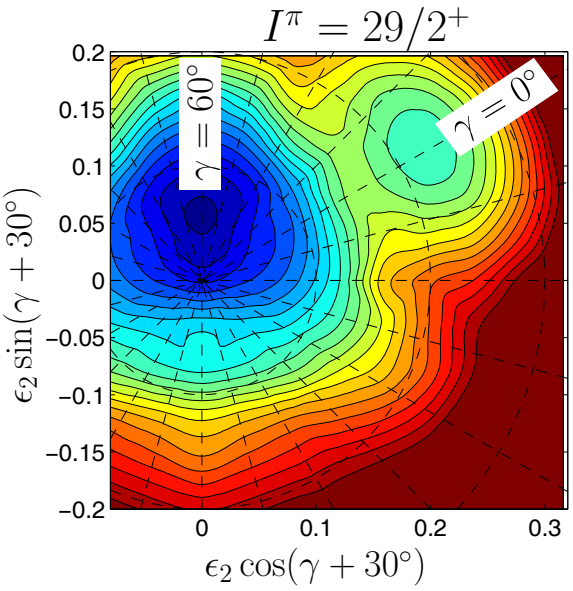

Fig. 17. The calculated potential energy surface for ^{87}Rb at $I = 29/2$ for the $(\pi,\alpha)_p(\pi,\alpha)_n = (+,1/2)(+,0)$ symmetry group. The contour line separation is 0.25 MeV.

the $5/2^-$ and $3/2^-$ states of ^{87}Rb and ^{89}Rb, this is not the case for ^{91}Rb.

5 Cranked Nilsson-Strutinsky-Bogoliubov calculations

For the $^{87}_{37}\mathrm{Rb}_{50}$ nucleus, extensive Cranked Nilsson-Strutinsky-Bogoliubov (CNSB) calculations were carried out. The calculations are based on a modified version of the code used in ref. [77]. The new code uses a different strategy which is described in detail in ref. [78]. The calculations were performed in a grid of eight parameters, namely the pairing parameters for protons and neutrons, (Δ_p, λ_p) and (Δ_n, λ_n), and the deformation parameters (ε_2, γ, ε_4), which are used as variational parameters, and the cranking frequency ω_x. For each set of variational parameters, all low-lying many-quasiparticle configurations were created using blocking, and traced diabatically [77] (removing virtual crossings) as a function of the cranking frequency ω_x. For each of these configurations, we performed particle-number projection and interpolated the projected energy as a function of ω_x to obtain values for fixed spins. In the final step of the calculation, the projected energy was minimized for each spin state ($I \approx I_x$) with respect to all configurations of a given symmetry and the variational parameters. (In this section, we choose to use I, rather than J, to denote the total angular momentum quantum number of a state.)

With the present method, information about individual configurations (occupancies of different orbitals) is lost but the advantage is that fully minimized yrast lines, corresponding to the 16 different parity and signature symmetry combinations, $(\pi,\alpha)_p(\pi,\alpha)_n$, can be obtained very efficiently in an automatic way. For selected $(\pi,\alpha)_p(\pi,\alpha)_n$ configurations, the energies from the calculation in the CNSB formalism for ^{87}Rb are shown in fig. 16. In these calculations, we have considered a (ε_2,γ)-mesh of 99 points shown in fig. 17, with a minimization also in 4 ε_4 points at each (ε_2,γ) deformation. Furthermore, no interpolation has been carried through in the 10 $\Delta_{p,n}$ and 7 $\lambda_{p,n}$ points; instead the $(\lambda_{p,n},\Delta_{p,n})$-mesh point giving lowest energy has been chosen. This is a more stable method but, with a limited number of points in the mesh, it can lead to some irregularities in the energy curves of fig. 16.

In the CNSB calculations for ^{87}Rb, we have used the "standard" [79] Nilsson single-particle parameters and for the rotating liquid drop energy, we have used the 1966 Myers-Swiatecki parameters [80] with the rigid-body moment of inertia calculated with a sharp surface with a radius parameter $r_0 = 1.2$ fm. For the pairing strength, we have used standard values specified in [77]. The CNSB calculations for ^{87}Rb, fig. 16, are in general agreement with observed yrast states, especially for states with $I < 10$. In both cases, one obtains irregular sequences of states typical for spherical or close-to-spherical deformations. Indeed, the yrast line up to $I \approx 20$ is calculated to be composed of close-to-spherical states having $\varepsilon_2 \simeq 0.05$. In fig. 16 we show only the yrast line for $(\pi,\alpha)_p(\pi,\alpha)_n = (+,\pm 1/2)(+,0)$ corresponding to the symmetry of the observed states, but the yrast line with opposite parity for the protons is also calculated to be close to spherical for $I < 20$ and to have about the same energy.

In fig. 16, the encircled points indicate states that are non-collective *i.e.* calculated to have $\gamma = 60°$ and thus correspond to terminating states. The first such point is obtained for $I = 9/2$ corresponding to one proton in the $1g_{9/2}$ orbital and four proton holes in the fp shell coupled to total angular momentum of zero. In order to get a better understanding of the terminating states, a comparison has been made with unpaired CNS calculations [79,81] where it is possible to fix configurations in terms of the number of particles in high- and low-j shells. In this way,

the favoured terminations seen at $I = 17/2$ and $I = 29/2$ can be understood as corresponding to configurations with one and three $1g_{9/2}$ protons, respectively. The $I = 29/2$ state and also the signature partner with $I = 27/2$ are calculated to be terminating states and are the highest spin states seen in experiment.

The energy surface drawn in fig. 17 for $I = 29/2$ shows both the terminating state and also a second more deformed minimum with $\varepsilon_2 \simeq 0.22$ and $\gamma = 0°$. The energy corresponding to the second minimum is also shown in fig. 16 where it is seen to become yrast around $I = 20$. A similar minimum is found with negative parity for protons and this energy is also displayed in fig. 16. However, these more deformed bands are calculated to be roughly 2 MeV higher in energy than the $I = 29/2$ state and are not seen, nor indeed expected to be seen, in the present experiment.

Calculations were also performed for the isotopes ^{89,91}Rb with similar results. In general, for the low-spin states we obtain weakly deformed yrast lines but where the additional neutrons added to the $2d_{5/2}$ shell drives the shape to slightly larger deformations, as discussed within the context of the Jahn-Teller effect in the introduction, sect. 1.

6 Summary

This paper is concerned with a study of the medium-high spin states of the rubidium isotopes ($Z = 37$) with $A = 87$, 89, and 91. Excited states were populated in binary transfer reactions initiated through the interaction of 530 MeV ^{96}Zr ions with a thin target of ^{124}Sn. Use of the Prisma/Clara setup in the measurements allowed the unambiguous identification of the projectile-like nuclei together with the associated γ rays. Data from a second experiment, which used the Gasp array to measure γ rays from the decay of fission fragments produced in the reaction ^{36}S + ^{176}Yb at 230 MeV, were used to build level schemes and to perform angular correlations measurements.

Experimental results have been compared with the results of spherical shell-model calculations, and cranked Nilsson-Strutinsky calculations. Shell-model calculations for ^{87}Rb and ^{89}Rb show a reasonably good agreement for the low- and most of the medium-spin states. Deviations between experiment and shell model for high-spin positive parity states of ^{87}Rb are possibly a consequence of the restricted shell-model space in the present work and may indicate the importance of crossing the neutron shell closure through *np-nh* neutron excitations for energies in excess of about 5 MeV. In ^{91}Rb it is possible, for each experimental state above the $9/2^+$ isomer, to identify an association of experimental and shell-model states but, given the number of relatively close lying high-spin shell-model states and the uncertainties in the experimental J^π values, the confidence in doing so is considerably reduced compared to the association for ^{87}Rb and ^{89}Rb. In this respect, further experimental work on the level structure of ^{91}Rb would be helpful.

Cranked Nilsson-Strutinsky calculations, including pairing, were performed to describe medium-spin states in the nuclei. The results confirm the spherical and close-to-spherical behaviour of ^{87,89,91}Rb. A very interesting second minimum is predicted for levels above the $29/2^+$ state; however, it was not possible to observe these levels in the present experiment and further experimental work is required to populate and study such non-yrast states.

The contribution of the accelerator and target-fabrication staff at the INFN Legnaro National Laboratory is gratefully acknowledged. We would also like to thank the scientific and technical staff at Legnaro National Laboratory who support the Gasp and Prisma/Clara arrays. RC and JFS acknowledge support from STFC through grants ST/L005808/1 and ST/P005101/1. DAT acknowledges support from Colciencias under contract 110165842984. This work was supported in part by the Academy of Finland and the University of Jyväskylä within the FIDIPRO programme. MHJ's work is supported by U.S. National Science Foundation Grant No. PHY-1404159.

Data Availability Statement This manuscript has no associated data or the data will not be deposited. [Authors' comment: All data generated during this study are contained in this published article.]

References

1. E. Margaret Burbidge, G.R. Burbidge, William A. Fowler, F. Hoyle, Rev. Mod. Phys. **29**, 547 (1957).
2. G.A. Jones, P.H. Regan, Zs. Podolyák, N. Yoshinaga, K. Higashiyama, G. de Angelis, Y.H. Zhang, A. Gadea, C.A. Ur, M. Axiotis, D. Bazzacco, D. Bucurescu, E. Farnea, W. Gelletly, M. Ionescu-Bujor, A. Iordachescu, T. Kröll, S.D. Langdown, S. Lenzi, S. Lunardi, N. Mărginean, T. Martinez, N.H. Medina, R. Menegazzo, D.R. Napoli, B. Quintana, B. Rubio, C. Rusu, R. Schwengner, D. Tonev, J.J. Valiente-Dobón, W. von Oertzen, Phys. Rev. C **76**, 054317 (2007).
3. D. Bucurescu, C. Rusu, N. Mărginean, C.A. Ur, G. de Angelis, L. Corradi, D. Bazzacco, S. Beghini, F. Della Vedova, G. Duchêne, E. Farnea, T. Faul, E. Fioretto, A. Gadea, W. Gelletly, B. Guiot, M. Ionescu-Bujor, A. Iordăchescu, S.D. Landown, S.M. Lenzi, S. Lunardi, P. Mason, C. Mihai, R. Mărginean, R. Menegazzo, G. Montagnoli, D. Napoli, Zs. Podolyák, P.H. Regan, F. Scarlassara, A.M. Stefanini, G. Suliman, S. Szilner, M. Trotta, J.J. Valiente-Dobón, Y.H. Zhang, Phys. Rev. C **76**, 064301 (2007).
4. N. Mărginean, D. Bucurescu, C.A. Ur, C. Mihai, L. Corradi, E. Farnea, D. Filipescu, E. Fioretto, D. Ghiţă, B. Guiot, M. Górska, M. Ionescu-Bujor, A. Iordăchescu, D. Jelavić-Malenica, S.M. Lenzi, P. Mason, R. Mărginean, D. Mengoni, G. Montagnoli, D.R. Napoli, S. Pascu, G. Pollarolo, F. Recchia, A.M. Stefanini, R. Silvestri, T. Sava, F. Scarlassara, S. Szilner, N.V. Zamfir, Phys. Rev. C **80**, 021301 (2009).
5. I. Ahmad, W.R. Phillips, Rep. Prog. Phys. **58**, 1415 (1995).

6. T. Rząca-Urban, K. Sieja, W. Urban, F. Nowacki, J.L. Durell, A.G. Smith, I. Ahmad, Phys. Rev. C **79**, 024319 (2009).
7. W. Urban, K. Sieja, G.S. Simpson, H. Faust, T. Rzaca-Urban, A. Złomaniec, M. Łukasiewicz, A.G. Smith, J.L. Durell, J.F. Smith, B.J. Varley, F. Nowacki, I. Ahmad, Phys. Rev. C **79**, 044304 (2009).
8. Peter Möller, J. Rayford Nix, At. Data Nucl. Data Tables **26**, 165 (1981).
9. D.A. Arseniev, A. Sobiczewski, V.G. Soloviev, Nucl. Phys. A **139**, 269 (1969).
10. E. Cheifetz, R.C. Jared, S.G. Thompson, J.B. Wilhelmy, Phys. Rev. Lett. **25**, 38 (1970).
11. J.H. Hamilton, A.V. Ramayya, S.J. Zhu, G.M. Ter-Akopian, Yu.Ts. Oganessian, J.D. Cole, J.O. Rasmussen, M.A. Stoyer, Prog. Part. Nucl. Phys. **35**, 635 (1995).
12. S. Naimi, G. Audi, D. Beck, K. Blaum, Ch. Böhm, Ch. Borgmann, M. Breitenfeldt, S. George, F. Herfurth, A. Herlert, M. Kowalska, S. Kreim, D. Lunney, D. Neidherr, M. Rosenbusch, S. Schwarz, L. Schweikhard, K. Zuber, Phys. Rev. Lett. **105**, 032502 (2010).
13. F. Buchinger, E.B. Ramsay, E. Arnold, W. Neu, R. Neugart, K. Wendt, R.E. Silverans, P. Lievens, L. Vermeeren, D. Berdichevsky, R. Fleming, D.W.L. Sprung, G. Ulm, Phys. Rev. C **41**, 2883 (1990).
14. C. Thibault, F. Touchard, S. Büttgenbach, R. Klapisch, M. de Saint Simon, H.T. Duong, P. Jacquinot, P. Juncar, S. Liberman, P. Pillet, J. Pinard, J.L. Vialle, A. Pesnelle, G. Huber, Phys. Rev. C **23**, 2720 (1981).
15. M. Keim, E. Arnold, W. Borchers, U. Georg, A. Klein, R. Neugart, L. Vermeeren, R.E. Silverans, P. Lievens, Nucl. Phys. A **586**, 219 (1995).
16. V.V. Simon, T. Brunner, U. Chowdhury, B. Eberhardt, S. Ettenauer, A.T. Gallant, E. Mané, M.C. Simon, P. Delheij, M.R. Pearson, G. Audi, G. Gwinner, D. Lunney, H. Schatz, J. Dilling, Phys. Rev. C **85**, 064308 (2012).
17. C. Sotty, M. Zielińska, G. Georgiev, D.L. Balabanski, A.E. Stuchbery, A. Blazhev, N. Bree, R. Chevrier, S. Das Gupta, J.M. Daugas, T. Davinson, H. De Witte, J. Diriken, L.P. Gaffney, K. Geibel, K. Hadyńska-Klęk, F.G. Kondev, J. Konki, T. Kröll, P. Morel, P. Napiorkowski, J. Pakarinen, P. Reiter, M. Scheck, M. Seidlitz, B. Siebeck, G. Simpson, H. Törnqvist, N. Warr, F. Wenander, Phys. Rev. Lett. **115**, 172501 (2015).
18. J.A. Pinston, J. Genevey, R. Orlandi, A. Scherillo, G.S. Simpson, I. Tsekhanovich, W. Urban, H. Faust, N. Warr, Phys. Rev. C **71**, 064327 (2005).
19. P.-G. Reinhard, E.W. Otten, Nucl. Phys. A **420**, 173 (1984).
20. W. Nazarewicz, Nucl. Phys A **574**, 27c (1994).
21. B. Pritychenko, M. Birch, B. Singh, M. Horoi, At. Data Nucl. Data Tables **107**, 1 (2016).
22. Y.H. Zhang, Zs. Podolyàk, G. de Angelis, A. Gadea, C. Ur, S. Lunardi, N. Mărginean, C. Rusu, R. Schwengner, T. Kröll, D.R. Napoli, R. Menegazzo, D. Bazzacco, E. Farnea, S. Lenzi, T. Martinez, M. Axiotis, D. Tonev, W. Gelletly, S. Langdown, P.H. Regan, J.J. Valiente-Dóbon, W. von Oertzen, B. Rubio, B. Quintana, N. Medina, R. Broda, Phys. Rev. C **70**, 024301 (2004).
23. A.M. Stefanini, L. Corradi, G. Maron, A. Pisent, M. Trotta, A.M. Vinodkumar, S. Beghini, G. Montagnoli, F. Scarlassara, G.F. Segato, A. De Rosa, G. Inglima, D. Pierroutsakou, M. Romoli, M. Sandoli, G. Pollarolo, A. Latina, Nucl. Phys. A **701**, 217 (2002).
24. S. Szilner, C.A. Ur, L. Corradi, N. Mărginean, G. Pollarolo, A.M. Stefanini, S. Beghini, B.R. Behera, E. Fioretto, A. Gadea, B. Guiot, A. Latina, P. Mason, G. Montagnoli, F. Scarlassara, M. Trotta, G. de Angelis, F. Della Vedova, E. Farnea, F. Haas, S. Lenzi, S. Lunardi, R. Mărginean, R. Menegazzo, D.R. Napoli, M. Nespolo, I.V. Pokrovsky, F. Recchia, M. Romoli, M.-D. Salsac, N. Soic, J.J. Valiente-Dobón, Phys. Rev. C **76**, 024604 (2007).
25. G. Montagnoli, A.M. Stefanini, M. Trotta, S. Beghini, M. Bettini, F. Scarlassara, V. Schiavon, L. Corradi, B.R. Behera, E. Fioretto, A. Gadea, A. Latina, S. Szilner, L. Donà, M. Rigato, N.A. Kondratiev, A.Yu. Chizhov, G. Kniajeva, E.M. Kozulin, I.V. Pokrovskiy, V.M. Voskressensky, D. Ackermann, Nucl. Instrum. Methods Phys. Res. A **547**, 455 (2005).
26. S. Beghini, L. Corradi, E. Fioretto, A. Gadea, A. Latina, G. Montagnoli, F. Scarlassara, A.M. Stefanini, S. Szilner, M. Trotta, A.M. Vinodkumar, Nucl. Instrum. Methods Phys. Res. A **551**, 364 (2005).
27. A. Gadea, D.R. Napoli, G. de Angelis, R. Menegazzo, A.M. Stefanini, L. Corradi, M. Axiotis, L. Berti, E. Fioretto, T. Kröll, A. Latina, N. Mărginean, G. Maron, T. Martinez, D. Rosso, C. Rusu, N. Toniolo, S. Szilner, M. Trotta, D. Bazzacco, S. Beghini, M. Bellato, F. Brandolini, E. Farnea, R. Isocrate, S.M. Lenzi, S. Lunardi, G. Montagnoli, P. Pavan, C. Rossi Alvarez, F. Scarlassara, C. Ur, N. Blasi, A. Bracco, F. Camera, S. Leoni, B. Million, M. Pignanelli, G. Pollarolo, A. DeRosa, G. Inglima, M. La Commara, G. La Rana, D. Pierroutsakou, M. Romoli, M. Sandoli, P.G. Bizzeti, A.M. Bizzeti-Sona, G. Lo Bianco, C.M. Petrache, A. Zucchiatti, P. Cocconi, B. Quintana, Ch. Beck, D. Curien, G. Duchêne, F. Haas, P. Medina, P. Papka, J. Durell, S.J. Freeman, A. Smith, B. Varley, K. Fayz, V. Pucknell, J. Simpson, W. Gelletly, P. Regan, the EUROBALL Collaboration, the PRISMA-2 Collaboration, Eur. Phys. J. A **20**, 193 (2004).
28. A. Latina, *Study of Heavy-Ion reactions with the Magnetic Spectrometer PRISMA*, PhD Thesis, Università Degli Studi di Torino (2004).
29. N. Fotiades, J.A. Cizewski, R. Krücken, R.M. Clark, P. Fallon, I.Y. Lee, A.O. Macchiavelli, D.P. McNabb, J.A. Becker, L.A. Bernstein, W. Younes, Phys. Rev. C **71**, 064312 (2005).
30. Giacomo de Angelis, Nucl. Phys. A **751**, 533 (2005).
31. D. Bazzacco and the GASP Collaboration, *The gamma ray spectrometer ga.sp*, in *Proceedings of the International Conference on Nuclear Structure at High Angular Momentum, Ottawa, Canada, AECL-10613* (IAEA, 1992) `https://inis.iaea.org/search/search.aspx?orig_q=RN:28057794`.
32. J. Ollier, R. Chapman, X. Liang, M. Labiche, K.-M. Spohr, M. Davison, G. de Angelis, M. Axiotis, T. Kröll, D.R. Napoli, T. Martinez, D. Bazzacco, E. Farnea, S. Lunardi, A.G. Smith, Eur. Phys. J. A **20**, 111 (2003).
33. M.A. Jones, W. Urban, W.R. Phillips, Rev. Sci. Instrum. **69**, 4120 (1998).
34. K.S. Krane, R.M. Steffen, R.M. Wheeler, At. Data Nucl. Data Tables **11**, 351 (1973).
35. B. Fornal, R.H. Mayer, I.G. Bearden, Ph. Benet, R. Broda, P.J. Daly, Z.W. Grabowski, I. Ahmad, M.P. Carpenter, P.B. Fernandez, R.V.F. Janssens, T.L. Khoo, T. Lauritsen, E.F. Moore, M. Drigert, Phys. Rev. C **49**, 2413 (1994).

36. J. Ollier, R. Chapman, X. Liang, M. Labiche, K.-M. Spohr, M. Davison, G. de Angelis, M. Axiotis, T. Kröll, D.R. Napoli, T. Martinez, D. Bazzacco, E. Farnea, S. Lunardi, A.G. Smith, F. Haas, Phys. Rev. C **71**, 034316 (2005).
37. X. Liang, R. Chapman, F. Haas, K.-M. Spohr, P. Bednarczyk, S.M. Campbell, P.J. Dagnall, M. Davison, G. de Angelis, G. Duchêne, T. Kröll, S. Lunardi, S. Naguleswaran, M.B. Smith, Phys. Rev. C **66**, 014302 (2002).
38. H. Takai, C.N. Knott, D.F. Winchell, J.X. Saladin, M.S. Kaplan, L. de Faro, R. Aryaeinejad, R.A. Blue, R.M. Ronningen, D.J. Morrissey, I.Y. Lee, O. Dietzsch, Phys. Rev. C **38**, 1247 (1988).
39. T.D. Johnson, W.D. Kulp, Nucl. Data Sheets **129**, 1 (2015).
40. O. Sorlin, M.-G. Porquet, Prog. Part. Nucl. Phys. **61**, 602 (2008).
41. J.F. Harrison, J.C. Hiebert, Nucl. Phys. A **185**, 385 (1972).
42. J.R. Comfort, J.R. Duray, W.J. Braithwaite, Phys. Rev. C **8**, 1354 (1973).
43. L.R. Medsker, H.T. Fortune, S.C. Headley, J.N. Bishop, Phys. Rev. C **12**, 1516 (1975).
44. P.C. Li, W.W. Daehnick, Swapan K. Saha, J.D. Brown, R.T. Kouzes, Nucl. Phys. A **469**, 393 (1987).
45. A. Shihab-Eldin, S.G. Prussin, F.M. Bernthal, J.O. Rasmussen, Nucl. Phys. A **160**, 33 (1970).
46. F.K. Wohn, J.K. Halbig, W.L. Talbert, J.R. McConnell, Phys. Rev. C **7**, 160 (1973).
47. P.D. Bond, G.J. Kumbartzki, Nucl. Phys. A **205**, 239 (1973).
48. L. Hulstman, H.P. Blok, J. Verburg, J.G. Hoogteyling, C.B. Nederveen, H.T. Vijlbrief, E.J. Kaptein, S.W.L. Milo, J. Blok, Nucl. Phys. A **251**, 269 (1975).
49. E. Barnard, D.W. Mingay, D. Reitmann, J.W. Tepel, Z. Phys. A **296**, 295 (1980).
50. L. Käubler, Ch. Protochristov, M. Michailova, J. Reif, W. Andrejtscheff, L. Funke, L. Kostova, H. Prade, R. Schwengner, G. Winter, Z. Phys. A **352**, 127 (1995).
51. L. Käubler, K.D. Schilling, R. Schwengner, F. Dönau, E. Grosse, D. Belic, P. von Brentano, M. Bubner, C. Fransen, M. Grinberg, U. Kneissl, C. Kohstall, A. Linnemann, P. Matschinsky, A. Nord, N. Pietralla, H.H. Pitz, M. Scheck, F. Stedile, V. Werner, Phys. Rev. C **65**, 054315 (2002).
52. M.M. Stautberg, J.J. Kraushaar, B.W. Ridley, Phys. Rev. **157**, 977 (1967).
53. A. Astier, M.-G. Porquet, Ts. Venkova, I. Deloncle, F. Azaiez, A. Buta, D. Curien, O. Dorvaux, G. Duchêne, B.J.P. Gall, F. Khalfallah, I. Piqueras, M. Rousseau, M. Meyer, N. Redon, O. Stézowski, R. Lucas, A. Bogachev, Eur. Phys. J. A **30**, 541 (2006).
54. Balraj Singh, Jun Chen, Nucl. Data Sheets **116**, 1 (2014).
55. E.C. May, S.A. Lewis, Phys. Rev. C **5**, 117 (1972).
56. A. Pfeiffer, G. Mairle, K.T. Knöpfle, T. Kihm, G. Seegert, P. Grabmayr, G.J. Wagner, V. Bechtold, L. Friedrich, Nucl. Phys. A **455**, 381 (1986).
57. P. Bączyk, W. Urban, D. Złotowska, M. Czerwiński, T. Rząca-Urban, A. Blanc, M. Jentschel, P. Mutti, U. Köster, T. Soldner, G. de France, G. Simpson, C.A. Ur, Phys. Rev. C **91**, 047302 (2015).
58. P.M. Endt, At. Data Nucl. Data Tables **23**, 547 (1979).
59. P.M. Endt, At. Data Nucl. Data Tables **26**, 47 (1981).
60. A. Astier, M.-G. Porquet, Ts. Venkova, G. Duchêne, F. Azaiez, D. Curien, I. Deloncle, O. Dorvaux, B.J.P. Gall, N. Redon, M. Rousseau, O. Stézowski, Phys. Rev. C **88**, 024321 (2013).
61. T. Pawłat, R. Broda, B. Fornal, W. Królas, J. Wrzesiński, R.V.F. Janssens, S. Zhu, M.P. Carpenter, W.B. Walters, N. Hoteling, Acta Phys. Pol. B **40**, 629 (2009).
62. E.A. Henry, W.L. Talbert, J.R. McConnell, Phys. Rev. C **7**, 222 (1973).
63. L. Corradi, G. Pollarolo, S. Szilner, J. Phys. G **36**, 113101 (2009).
64. D.A. Torres, R. Chapman, K.-M. Spohr, J.F. Smith, V. Kumar, A. Hodsdon, X. Liang, R. Orlandi, P. Wady, Z. Wang, M. Labiche, D. O'Donnell, J. Ollier, D. Bazzacco, S. Beghini, E. Farnea, R. Mărginean, D. Mengoni, G. Montagnoli, F. Recchia, F. Scarlassara, C.A. Ur, S. Lunardi, T. Kröll, A. Gottardo, S. Aydin, L. Corradi, E. Fioretto, A. Gadea, G. de Angelis, N. Mărginean, D.R. Napoli, R. Silvestri, A.M. Stefanini, S. Szilner, J.J. Valiente-Dobón, F.D. Vedova, M. Axiotis, T. Martinez, S.J. Freeman, A.G. Smith, G. Jones, N. Thompson, F. Haas, F. Tatjana, in *AIP Conference Proceeding: Proceeding of the 4th International Workshop on Nuclear Fission and Fission-Product Spectroscopy* (AIP, 2010).
65. W. Urban, J.L. Durell, A.G. Smith, W.R. Phillips, M.A. Jones, B.J. Varley, T. Rząca-Urban, I. Ahmad, L.R. Morss, M. Bentaleb, N. Schulz, Nucl. Phys. A **689**, 605 (2001).
66. J.K. Hwang, A.V. Ramayya, J.H. Hamilton, S.H. Liu, K. Li, H.L. Crowell, C. Goodin, Y.X. Luo, J.O. Rasmussen, S.J. Zhu, Phys. Rev. C **80**, 037304 (2009).
67. G.S. Simpson, W. Urban, K. Sieja, J.A. Dare, J. Jolie, A. Linneman, R. Orlandi, A. Scherillo, A.G. Smith, T. Soldner, I. Tsekhanovich, B.J. Varley, A. Złomaniec, J.L. Durell, J.F. Smith, T. Rząca-Urban, H. Faust, I. Ahmad, J.P. Greene, Phys. Rev. C **82**, 024302 (2010).
68. Coral M. Baglin, Nucl. Data Sheets **114**, 1293 (2013).
69. K. Sistemich, K. Kawade, H. Lawin, G. Lhersonneau, H. Ohm, U. Paffrath, V. Lopac, S. Brant, V. Paar, Z. Phys. A **325**, 139 (1986).
70. E. Achterberg, F.C. Iglesias, A.E. Jech, J.A. Moragues, D. Otero, M.L. Pérez, A.N. Proto, J.J. Rossi, W. Scheuer, Phys. Rev. C **9**, 299 (1974).
71. O.V. Bespalova, T.A. Ermakova, E.A. Romanovskii, T.I. Spasskaya, A.A. Klimochkina, Bull. Russ. Acad. Sci. Phys. **73**, 816 (2009).
72. M. Hjorth-Jensen, T.T.S. Kuo, E. Osnes, Phys. Rep. **261**, 125 (1995).
73. D.R. Entem, R. Machleidt, Phys. Rev. C **68**, 041001 (2003).
74. S.K. Bogner, T.T.S. Kuo, A. Schwenk, Phys. Rep. **386**, 1 (2003).
75. E. Chabanat, P. Bonche, P. Haensel, J. Meyer, R. Schaeffer, Phys. Scr. **T56**, 231 (1995).
76. Takaharu Otsuka, Toshio Suzuki, Rintaro Fujimoto, Hubert Grawe, Yoshinori Akaishi, Phys. Rev. Lett. **95**, 232502 (2005).
77. T. Bengtsson, Nucl. Phys. A **496**, 56 (1989).
78. B.G. Carlsson, I. Ragnarsson, R. Bengtsson, E.O. Lieder, R.M. Lieder, A.A. Pasternak, Phys. Rev. C **78**, 034316 (2008).
79. Tord Bengtsson, Ingemar Ragnarsson, Nucl. Phys. A **436**, 14 (1985).
80. W.D. Myers, W.J. Swiatecki, Ark. Phys. **36**, 343 (1967).
81. B.G. Carlsson, I. Ragnarsson, Phys. Rev. C **74**, 011302 (2006).